NJF Seminar 438: Automatic GNSS referred image acquisition in field experiments

Green, Ole; Jørgensen, Rasmus Nyholm

Published in:
NJF Report

Publication date:
2010

Document version:
Final published version

Citation for pulished version (APA):
Green, O., & Jørgensen, R. N. (2010). NJF Seminar 438: Automatic GNSS referred image acquisition in field experiments. *NJF Report*, *6*(7), 71-72.

NJF Report • Vol 6 • No 7 • Year 2010

Nordic Association of Agricultural Scientists

NJF Seminar 438

Sensors for soil and plant mapping and terrain analysis

Skara, Sweden, 27-28 October 2010

NJF
Nordic Association of Agricultural Scientists

SLU

Contents

Preface

The present publication is a compilation of the abstracts for the NJF seminar 438: *Sensors for soil and plant mapping and terrain analysis*, in Skara, Sweden, 27-28 October 2010. The objective of the seminar is to present a variety of measurement techniques and their applications to provide an opportunity for knowledge exchange and discussion concerning the use of sensors for soil and plant mapping, terrain analysis and other related subject areas.

The organizing committee consisted of Anton Gårde Thomsen, Ole Green and Claus Aage Grøn Sørensen, Aarhus University, Denmark, Tiit Plakk, Estonian Research Institute of Agriculture, Estonia, Stein Ivar Øvergaard, Bioforsk, Norway and Bo Stenberg and Kristin Piikki, SLU, Swedish University of Agricultural Sciences, Sweden.

Bo Stenberg and Kristin Piikki

Skara, October 2010

Sensors based on soil electrical properties

Tiit Plakk

Estonian Resaerch Institute of Agriculture,Saku, Teaduse 13, Estonia.

Corresponding author, Phone: +3725511051, E-mail: tiit.plakk@eria.ee

The measurement is important to get reliable, plausible and comparable data about the real world we are living in. The most important part of every measurement system is sensor, the front end of a device where happens the interaction between measurement signal and material under test. The modern world of different sensors used in agriculture and near fields is huge and complicated. Just to name some commonly used electrical probes, instruments and methods on the market for soil study: Acclima, Aquaflex ,Theta Probe, Hydra Probe, TDR100, Textronix TDR, CS-616, ECH20, EC20, 5TE, Enviroscan, GPR solutions, Moisture Point, Watermark, Thermal Conductivity Sensor, Percometer, TDR Field Scout, Aqua Boy, WET probe, Tramex, Testo, TDR Trase, EM38 (Induction), Veris 3100 System (contact) Wiener array system, remote sensing active and passive radiometry.

Fig.1. Some soil sensors:(A) time domain reflectometer, (B) ECH2O EC-20 probe, (C) Hydra probe,(D) Acclima time domain transmission sensor, (E) ThetaProbe, (F) CS-616. The center figure shows a cart-mounted ground penetrating radar (GPR); the right figure is a passive microwave remote sensing radiometer mounted on a crane. (Robinson et al., 2008)

All these instruments are electrical indirect measurement systems where some amount of electrical energy is induced by different means into the material and the response signal of the material is measured. The frequency of used electrical signal varies from DC to tenth of GHz and in shape from sine wave to sharp edged pulse signals. The response signal is always determined by material electrical properties.

Material electrical properties.

Material electrical properties are characterized by the complex permittivity ε^*, expressing the material's response to the polarizing effect of an applied electric field. The permittivity is defined as relation between the electric flux density D and electric field intensity E applied to the material as: $D=\varepsilon^*E=(\varepsilon'-j\varepsilon'')E$ The complex dielectric constant or relative permittivity ε^*_r (sometimes referred also as k^*) is the ratio of the permittivity of a medium ε^* to that of a vacuum ε_0 :

$\varepsilon^*_r = \varepsilon^*/\varepsilon_0 = (\varepsilon'-j\varepsilon'')/\varepsilon_0 = \varepsilon'_r - j\varepsilon''_r$ where ε'_r is the real part of dielectric constant and represents the ability of material to store energy by polarization effect and ε''_r is the imaginary part of dielectric constant which is the measure of electrical losses. The study and understanding of both energy storing and loss mechanism is the core of dielectric theory for sensor application. The loss tangent $\tan\delta = \varepsilon''/\varepsilon'$ indicates the „lossiness" of a material and equals to the ratio of the energy lost to the energy stored. The loss tangent is an important parameter of a material on a certain frequency and determines the possibility of veridical measurement of ε'_r by a given measurement method.

Dielectric losses include losses due to molecular relaxation and ionic conduction (σ) and are given by von Hippel, (1954) as: $\varepsilon''_r = \varepsilon''_{r\,mr} + \sigma/\omega\varepsilon_0$ For frequencies much less than relaxation frequency (17 GHz for free water) relaxation losses can be neglected and we can write: $tan\delta = \varepsilon''/\varepsilon' = \sigma/\omega\varepsilon_0\varepsilon' = I_r/I_c = 1/Q$ where I_r and I_c are conductivity and shift currents in the material and Q is quality factor. (Agilent, 2006)

The complex dielectric permittivity is frequency and temperature dependent and for many materials may be described by Cole-Cole (1941) model

$$\varepsilon_r(f,\mathrm{T}) = \varepsilon_\infty + \frac{\varepsilon_s(\mathrm{T}) - \varepsilon_\infty}{1 + j\left(\frac{f}{f_{rel}(\mathrm{T})}\right)^{1-\beta}} - \frac{j\sigma_{dc}(T)}{2\pi f\varepsilon_0}$$

where ε_∞ is the dielectric constant at infinite frequency (optical), ε_s the static dielectric constant at f=0 (DC) Hz and β a factor accounting for possible spread in relaxation frequencies.

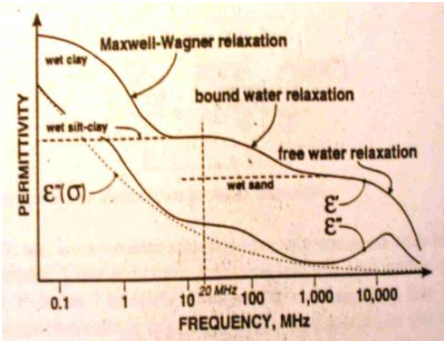

Fig. 2. Frequency response of dielectric mechanisms of wet soils (de Loor, 1983)

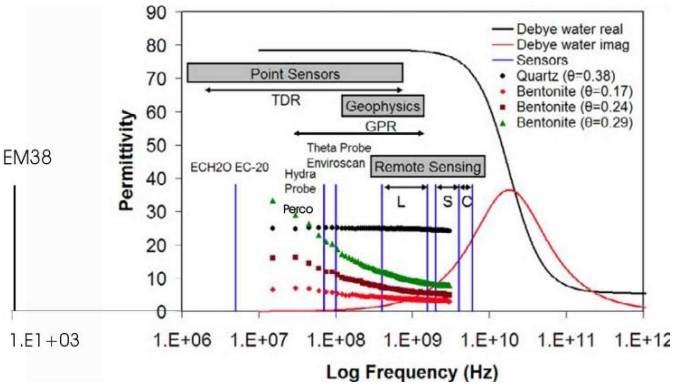

Fig.3. Dielectric data for quartz sand with no dielectric dispersion and moist clays showing dielectric dispersion; the real and imaginary permittivity for water without ionic conductivity are indicated for reference. The frequency ranges of sensors from Fig 1 are indicated, modified from Robinson et al., 2008.

Soil electrical properties for measurement application

Dielectric constant of free water ε'_r of water is 80.2 at 20 ^{0}C with temperature coefficient -0.37 $^0C^{-1}$ and remains nearly constant in whole frequency range of interest. (Kaatze, 2005) The frequency dependence of ε^*_r is presented by Debye equation whereas the relaxation frequency is 17 GHz, which is outside the frequency range of commonly used sensors

Dielectric properties of bound water of 1-10 molecular layers differs significantly from free water, has frequency dispersion at frequencies below 1 GHz and is in range 3…10 (30). (Boyarskii et al., 2002, Saarenketo, 1998). The influence of bound water on bulk electrical properties is small for sandy soil and increases with clay content. The dielectric behavior of bound water is complicated and still to be researched.

The ε'_r of most dry materials in soil is 3…7 and does not have significant frequency dispersion in interesting us frequency range with exception of clay minerals. Soil is a

3 component dielectric mixture of air, water and solid phase. In literature a number of well-known formulas exist to calculate electrical properties of mixture from the volume fractions and electrical properties of the constituents. This complicated by electrical behavior of different state of water in soils. The measurement by interaction of electric field and a certain amount of soil around probes has inherited statistical nature due to shape and distribution of particular components. The resulting dielectric constant is different for parallel and in series alignment of dielectric layers of the same amount. One of the widely used formulas for multiphase dielectric mixtures is complex refractive index model CRIM (Birchak, 1974)

$$\sqrt{\varepsilon^*_m} = \sum_{i=1}^{n} f_i \sqrt{\varepsilon^*_i}\ )$$

where ε^*_m , V_i and ε^*_i are the resulting dielectric constant, volume fraction and constituents dielectric constant. More general equation is derived from Lichtenecer-Rother theory, where the exponent ½ in CRIM is replaced by shape factor *c* between -1 and 1. The *c* is found to be around 0.5 (CRIM) for variety of soils. Modern theories consider the soil as 4 component mix adding bound water volume as a separate component.

Soil bulk dielectric constant ε'_a is mainly defined by soil volumetric water content θ whereas the shape of the curve ε'_a (θ) depends on soil texture. For a variety of mineral soils in frequency range 10 Mhz…1 GHz this relationship can be approximated by empirical Topp equation (Topp et al., 1980):

$\varepsilon'_a = 3.03 + 9{,}3\,\theta + 146\,\theta^2 - 76.7\,\theta^3$. This relationship is widely used by equipment manufactures as general calibration curve for dielectric soil moisture measurement instruments.

For most soils up to 100 MHz…1GHz the electrical losses ε''_r are determined by ionic conductivity; only in heavy clays different dielectric loss mechanism have some importance (Saarenketo, 1998, de Loor, 1984). The apparent ionic conductivity EC_a, frequently measured by instrument EM38 is often used for mapping of variety of soil properties that influence the yield.(Corwin, Lesch, 2005). Although the EC_a is formed by a number of different soil parameters the most important is combination of soluble salts and soil moisture and in less extent clay and organic matter content. The soil salinity is defined as the electrical conductivity of saturated soil extract EC_e at 25 or 20 C^o and the numerical values are the basics of soil salinity classifications.(USDA 1954). One of the key problems of interpretation of EC_a measurement is to translate the EC_a values into comparable EC_e values. Rhoads et al. (1999) have raised an extensive research on soil EC mechanisms and present formulas of EC_a-EC_e relationship. These formulas contain a lot of difficult to get parameters like the volume of continuous water pathways and soil surface area with the bound water fraction. In practice soil with EC_a = 0.5 dS/m can be heavily salt affected if the θ is small and non salty normal soil if θ is near the field capacity.

Hence in a large scale the ε'_r depends only on water content and ε''_r (EC_a) depends substantially both on water content and soluble salts the simultaneous measurement of ε'_r and EC_a yields more complete information about soil moisture and salinity. In case of non salty soils the soil EC_e is a good indication of nutritional elements in soil (Kadaja et al., 2009). The ε'_r measurements along with EC_a measurement by EM38 or other similar instruments enables better interpretation of EC_a results. Hilhorst (2000) has presented a theory and instrument for determination of the pore water conductivity from the measurements of soil complex dielectric constant.

The physical mechanism behind the water-solid interaction which influences the apparent ε'_r and soil water matrix potential are both related to surface forces limiting the water dipole movement ability. The soils ε'_r is a more complete indication of soil water availability to plants than just the water content. There is also an hypothesis (Plakk, 1988) that the dielectric constant of the soil water at biologically optimum

water content range for plants is in some extent smaller than ε'_r of free water indicating, that water is weakly bound to soil matrix.

Measurement methods of electrical sensors

The soil electrical parameters (complex dielectric constant) can be measured:

Frequency Domain (FD), where the probe with material forms electrical capacitor and by electronic means the change of capacitance due to the material is measured. Another variation of FD method is transmission line technique, where the probe is considered as a transmission line which characteristic impedance depends on surrounding media.

Time-Domain. A sharp electrical impulse is fed into the material thru contact electrodes and the reflected signal is measured and analyzed, (reflectometry, TDR) or the signal transmission time is measured (TDT)

Ground Penetrading Radar (GPR). The energy pulse is fed into the ground thru antenna system near the surface and the received signal is analyzed in terms of time and shape. The signal velocity depends on soil dielectric constant and the attenuation depends on electrical losses.

Remote sensing. The antenna systems from space or planes send out signals in different frequency bands and the reflections are received and analyzed. Passive remote sensing relies on measurement of soil emission in different spectral ranges. (Robinson et al., 2008).

All these instruments and methods use conversion calculation to convert electrical values into moisture or other parameters of interest, but usually they do not present directly the electrical properties of material. This adds an error into the interpretation of measurement result: its not possible to distinct between the uncertainties from measurement system and conversion calculation.

Soil conductivity is measured on low frequency with induction type (EM38, 14.5 kHz) or direct contact systems (Veris 3100, variety of point meters) with low frequency alternating current or by TDR thru sophisticated waveform analyzes (Robinson et al, 2003)

The influence of conductivity on measurement frequency

Electrical conductivity EC_a prescribes the minimum measurement frequency of TD instruments and the applicability of TD and radar systems. Its obvious, that if EC_a is very high the signal is short circuited and no measurement is possible. Every electrical method used at FD instruments has maximum aloud value of electrical losses $\tan\delta = 1/Q$. The well known resonant method requires quality factor $Q>30$ of a tuned tank circuit to get reliable results, i. e. $\tan\delta<0.03$. More advanced measurement methods aloud $\tan\delta$ up to 1…3 to get plausible ε'_r values. Even in case of a low conductivity soil EC_a=0.01 S/m the ε''_r =178 at frequency 1 MHz resulting in $\tan\delta\approx10$ (at average moisture content ε'_r=17.8) which is far beyond of FD system measurement capability. Because of soils electrical conductivity it is not possible to use the dielectric measurement method for soils at frequencies below 10 MHz. From other hand at higher frequencies the dispersion emerges depending on material texture (mainly clay and organic matter content). In practice the frequency range 30-100 MHz is used for FD instruments.

However, there are different allegedly dielectric instruments operating in lower frequency region. These "dielectric" measurements are mostly affected by material conductivity, various double layer structures between the probe and material interfaces etc. in a mixed form. The term "bulk dielectric constant" at low frequencies is disputable – what do we account into this term? The electrical capacity of a measurement cell due to material ε'_r is in the range of picofarads, but the double layers between soil particles or at metal electrode surface can cause the capacity in

the range of microfarads/cm^2 and they do not characterize the material bulk properties.

Electrical losses hinder also applicability of TD and radar systems because of signal attenuation and shape distortion below measurable levels. The interpretation of TD signals is complicated, because the initial signal is a sharp pulse, which contains a wide frequency spectra. However, it has been demonstrated that the electrical properties measured by FD and TD instruments are comparable (Robinson et al., 2003, Heimovaara et al., 1996)

Conclusion

All electrical sensors and measurement methods are based on electrical properties of material, which is described as material complex dielectric constant. The last consists of real part ε'_r (energy storage, electrical capacity, mainly determined by soil water) and imaginary part ε''_r (energy dissipation, electrical conductivity, mainly determined by soluble salts and water content). Soil ε''_r is caused by ionic conductivity and different dielectric loss mechanisms must be considered while choosing the measurement methods and analyzing of results. The best information about material is acquired by determination of dielectric constant and conductivity simultaneously. The reported only values of soil EC_a can not be used for extensive analyses and exploited in other region unless the moisture values or even better, ε'_r is also presented. Irrespective of the great amount of sophisticated dielectric theories the best way to convert soil electrical values into moisture and salinity content is to use specific calibration curves. The dielectric behavior of moist materials is complicated and needs further research in order to enhance the measurements and understanding of electromagnetic processes on materials.

References

Agilent 2006. Basics of Measuring the Dielectric Properties of Materials. Application Note. cp.literature.agilent.com/litweb/pdf/5989-2589EN.pdf

Birchak, J.R., Gardner, C.G, Hipp, J.E., Victor, J.M.,1974. High Dielectric Constant Microwave Probe for Sensing Soil Moisture, Proceeding of the IEEE, 62, pp.93-98

Boyarskii, D.A., Tikhonov, V.V., Komarova, N.Yu., 2002. Model of dielectric constant of bound water in soil for applications of microwave remote sensing. J. Electromagnetic Waves Appl 16:411–412.

Cole, K.S. Cole, R.H., 1941. Dispersion and adsorption in dielectrics alternating current characteristics. Journal of Chemical Physics. 9:p.341-351.

Corwin, D.L., Lesch, S.M., 2005. Apparent soil electrical conductivity measurements in agriculture. Computers and Electronics in Agriculture 46 p. 11–43

de Loor, G.P., 1983. The dielectric properties of wet materials. IEEE Transactions of Geosci- ence and Remote Sensing GE-21364-369

Heimovaara, T.J., de Winter, E.J.G, van Loon W.K.P, Esveld, D.C., 1996. Frequency-dependency dielectric permittivity from 0 to 1 GHz: Time domain reflectometry measurements compared with frequency domain network analyzer measurements, Water Resour. Res., 32, 3603 – 3610.

Hilhorst, M.A., 2000. A pore Water Conductivity Sensor, Soil Sci. Am. J, vol. 64, pp. 1922–1925.

Kaatze, U., 2005. Electromagnetic Wave Interactions with water and Aqueous Solutions. p.15-37. In: Kupfer, K. (Ed.). Electromagnetic aquametry: electromagnetic wave interaction with water and moist substances. Springer Berlin Heidelberg New York.

Kadaja, J. Plakk, T., Saue, T., Nugis, E., Viil, P., Särekanno, M., 2009. Measurement of soil water and nutrients by its electrical properties. Acta Agriculturae Scandinavica: Section B, Soil and Plant Science, 59, 447 - 455.

Plakk, T., 1990. Correlation Between Availability of Moisture to Plants and dielectric constant of soil. – Sov. Soil Sci. 22/ 21, pp 98–105, Washington, Scripta Publications.

Rhoades, J.D., Chanduvi, F., Lesch, S., 1999. Soil Salinity Assessment: Methods and interpretation of electrical conductivity measurements. FAO Irrigation and Drainage paper 57, Rome, Italy. ISSN 0254–5284.

Robinson, D.A., Campbell, C.S., Hopmans, J.W., Hornbuckle, B.K., Jones, S.B., Knight R., Ogden F., Selker J., Wendroth O.,2008. Soil Moisture Measurement for Ecological and Hydrological Watershed-Scale Observatories: A Review. Vadose Zone J. 7:358–389 Vol. 7.

Robinson, D.A., Jones, S.B., Wraith, J.M., Or D., Friedman, S.P., 2003. A review of advances in dielectric and electrical conductivity measurement in soils using time domain refectometry. Vadose Zone J. 2:444–475.

Saarenketo, T., 1998. Electrical Properties of Water in Clay and Silty Soils. Journal of Applied Geophysics 40 (1—3): 73—88

Topp, G.C., Davis J.L,. Annan A.P., 1980. Electromagnetic determination of soil-water content measurements in coaxial transmission-lines. Water Resour. Res. 16:574–582.

USDA 1954. Diagnosis and improvement of saline and alkali soils. Agriculture Handbook 60., Washington DC.

von Hippel, A. R., 1954. Dielectric Materials and Applications. John Wiley & Sons, Inc., New York.

Mapping variation in soil and plant properties in Norway – Experiences from the last decade

Audun Korsaeth[*] and Stein Ivar Øvergaard

Norwegian Institute of Environmental and Agricultural Research,Bioforsk Arable Crops Department, N-2849 Kapp, Norway,

**) Corresponding author, Phone: +47 40482560, Fax: +47 61160313, E-mail: audun.korsaeth@bioforsk.no*

Introduction

Precision agriculture is dealing with the within-field variation of soil and plant properties, where a tailored treatment of soil and plant should increase the efficiency of the input factors. Such an increase would lead to improved economical return for the farmer and reduced environmental impact. A pre-requisite for precision agriculture is sufficient and robust data on the spatial (and temporal) distribution of key parameters of soil and plants governing the agronomic management. A wide pallet of sensors offers a time- and cost-efficient approach to gather such data. In this paper, we will sum up some of our experiences with the use of selected sensors under Norwegian conditions.

Material and methods

Sensor for mapping variation in soil properties

A well established sensor-based technique to map soil variation is to measure apparent electrical conductivity (EC_a) of a soil profile. This may be performed in different ways, such as the electromagnetic induction (EM) approach. The device selected for our measurements was the Geonics EM38 (Mississauga, ON, Canada; www.geonics.com), which is the EM-EC_a sensor most often used in agricultural application. The device has an intercoil spacing of 1 m and may be operated in one of two measurement modes. In vertical mode (coil axes perpendicular to soil surface, EM_V) the effective measuring depth is approximately 1.5 m, whereas in horizontal mode (coil axes parallel to soil surface, EM_H) the effective measuring depth is approximately 0.75 m.

Sensors for mapping variation in plant properties

Measuring spectral reflectance is probably the mostly used remote sensing approach in agriculture. We have gathered experience with two hand-held point spectroradiometers: a CropScan instrument (version MSR16R, CropScan Inc., USA, www.cropscan.com) with 13 photodiodes (485-1650 nm), and a 2150-channel FieldSpec3 instrument (version 3, Analytical Spectral Devices Inc., USA, www.asdi.com, 350-2500 nm). Additionally, we have worked with an airborne hyperspectral line scanner (HySpex VNIR-1600, Norsk Elektro Optikk AS, Norway, www.neo.no), with 160 image wavelength layers (400-1000 nm), and with a pixel size of 20x20 cm on the ground from 1000 m flight altitude.

Measurements and model development

Sensor measurements have been performed on normally managed fields, on-going field trials and for the purpose constructed field trials. A total of about 600 ha have been mapped by the EM38 in the period, covering the most typical agricultural soils in Norway. Spectral reflectance has been measured on many crops, but most intensively on spring barley, spring wheat and winter wheat. The sensors have been tested by comparing their respective measurements with traditional laboratory analyses taken on soil/plant samples obtained from the areas measured by the sensors. Typically, a part of the data has been used for calibrating models (MLR-, PLS- and/or PPLS-models), whereas the remaining data has been used for validation.

Results and discussion

Mapping variation in soil properties

Measurements performed with the EM38 in horizontal mode (EM_H) were overall stronger correlated to measured top-soil properties than corresponding measurements in vertical mode (EM_V). In most cases, this was also valid for sub-soil properties. Hence, EM_H became the preferred mode of operation in all studies presented here.

On a 15 ha field with clay soil in S Norway (59°17'N, 10°22'E, 50 masl), a field survey was conducted in 2002 (Korsaeth, 2004). Measurements of EM_H-EC_a were significantly ($p \leq 0.05$) correlated with most of the measured variables of the topsoil, except P-AL, total N and organic C. They explained 63, 75 and 88 % of the variation in clay content, Mg-AL and exchangeable K, respectively. High correlation between EC_a and clay content is commonly found, and may partly be explained by the exchangeable cations associated with clay minerals, which represent an important pathway for EC in soil (Corwin and Lesch, 2003). In this study there was a high correlation between clay content and Mg and K ions.

Another study was performed in 2002 on two locations with morainic soils (Bioforsk Apelsvoll: 60°42'N, 10°51'E, 250 masl, and the long-term experiment at Møystad: 60°47'N, 11°10'E, 150 masl) (Korsaeth, 2008). As for the clay soil, measurements of EM_H-EC_a were correlated with many of the measured soil properties. Here, strongest correlation was found with topsoil clay and sand content. Regression analyses showed that up to 89% of the variation in measured EC_a could be explained by the variation in a selection of soil properties.

Soil texture, is however, not always well correlated with EC_a. On a 32 ha large morainic field (60°50'N, 11°18'E, 315 m above sea level), typical for the higher regions around lake Mjøsa, characterized by large topographic variation and the occurrence of peaty areas, EM_H-EC_a was best correlated with cation exchange capacity (r=0.84), soil water content (r=0.84), and ignition loss (r=0.83) (Korsaeth et al., 2008). In contrast to the other locations described above, measured EC_a-EM_H was unaffected by the clay content. This finding is quite untypical. As already mentioned, high correlations between EC_a and clay content may partly be explained by the exchangeable cations associated with clay minerals. In the current study there was a very strong correlation between EC_a and CEC, but clay content was not correlated with the exchangeable cations. CEC was, however, strongly correlated with SOM (r=0.918). In general, it appears that the EM_H-EC_a measurements are strongest correlated with the soil property which shows the largest variation within the measured field, and which represent a pathway for EC in soil.

In the latter study (Korsaeth et al., 2008) the standard procedure used for commercial soil survey in Norway (EM_H-EC_a method) was tested. Such a survey normally ends up with a color map, showing zones with different conductivity. The results showed that there were significant differences in soil organic matter (SOM) content between all seven zones tested, and it was concluded that the survey method may provide maps which shows significant differences in soil properties.

Interestingly, the EM_H-EC_a approach may also be used to detect variations in inorganic soil N content (cN_{inorg}). This was tested in spring barley during two cropping seasons (2002 and 2003) at two sites with morainic loam in SE Norway (Bioforsk Apelsvoll and Kise Research Station: 60°46'N, 10°48'E, 130 masl) (Korsaeth, 2005a). The experiment was constructed to maximize soil variation, and comprised five N level treatments: 0, 60, 90, 120 and 150 kg N ha^{-1}. In spite of the noise caused by the soil heterogeneity, concentrations of cN_{inorg} or NO_3-N were most strongly correlated with EC_a in both years and at both locations. The measurements of EC_a reflected well the temporal variation in inorganic N content, and a ranking of the treatments based on EC_a fitted very well with a ranking based on cN_{inorg} at the first

three sampling times after fertilizing. It was concluded that the method of using EC_a appears to be quite robust in terms of detecting relative differences in $cN_{inorg,}$ whereas a determination of absolute levels of cN_{inorg} with the method is unreliable.

Mapping variation in plant properties

A system for effective classification of agricultural crops would improve the quality of early yield estimates, since current information on the size of area sown with different crops tend to be relatively late available. Frequent clouds during the cropping season poses a challenge to satellite based methods in Norway. In a study performed in 2004 (Korsaeth and Ørka, 2007), we tested the potential of using an airborne hyper-spectral imager (HySpex) for crop classification under Norwegian conditions. Data was acquired by flying over the cropping system experiment at Bioforsk Apelsvoll in the end of June. The experiment consists of 48 plots (15 x 30 m large), covering spring (s.) barley, s. wheat, oats, potato and different kinds of grassland, and with a range of fertilizer regimes including organic and conventional cropping, with and without animal manure. The producer accuracy for the classes s. wheat, oat, s. barley and potato were 0.90, 0.28, 0.99 and 0.88, respectively. The corresponding user accuracies were 0.82, 1.00, 0.79 and 0.97. With the exception of oats and the heterogeneous group of grasslands, the crops were thus well classified from the multi-spectral data obtained just before shooting of the cereals.

Information on single crop properties such as plant N-content and above-ground biomass are of interest for management decisions (e.g. presicion fertilization), if available early enough in the season. In another study performed in 2004 (Korsaeth, 2005b), we tested whether data obtained in June with the handheld CropScan could be used to predict such properties, in addition to predictions of yields and protein concentration at harvest (August). Measurements were performed in winter wheat and spring barley in two ongoing fertilizer experiments. For winter wheat, regression models predicted up to 55, 89, 88 and 28% of the variations in N-content, biomass, yields and protein content, respectively. For spring barley the corresponding predictions were 87, 96, 87 and 22 %. Although the results were promising for N-content, biomass and yields, protein content at harvest was poorly predicted in both cereals.

In a more recent study on spring wheat (Øvergaard et al., 2010), comparing the instruments CropScan, FieldSpec3 and HySpex, we were, however, able to predict the grain protein content very well too. A spring wheat field experiment of 160 plots was measured five times during the 2007 growing season. At harvest, grain yield was measured on each plot and analyzed for moisture, protein, gluten, starch concentration and Zeleny sedimentation value. The predictive performance of the calibrated models was very good, with coefficients of determination for the validation data (R^2_{pred}) reaching 0.97 and 0.94 for grain yield and grain protein concentration, respectively. The predictions (R^2_{pred}) of the other grain quality variables were in the range of 0.88-0.92. A PPLS variable selection was carried out on the FieldSpec3 data, which reduced the analyzed data set from 975 to 3-5 wavelengths. Although the number of retained variables was very low, the reduced models still had almost the same predictive ability as the PPLS models based on the full data set.

Outlook

Numerous studies have shown that various sensor based approaches provide cost effective systems for mapping variation in a range of soil and crop properties. Some of these studies have resulted in commercial products, which are commonly using a tractor as platform for data acquisition. The rapid development of lightweight sensors, unmanned aerial vehicles (UAVs) and robots now opens for a new generation of products suited for site-specific management at farm level. The challenge to fill the gap between technology and agronomy is, however, larger than ever.

References

Corwin, D.L., Lesch, S.M., 2003. Application of Soil Electrical Conductivity to Precision Agriculture: Theory, Principles, and Guidelines. Agronomy Journal 95, 455-471.

Korsaeth, A., 2004. Relations Between Electrical Conductivity, Soil Texture and Chemical Properties on a Clay Soil in S Norway. Published in: Conference Abstracts of the Seventh International Conference on Precision Agriculture, July 25-28, Minneapolis, USA., p. 195.

Korsaeth, A. 2005a. Soil apparent electrical conductivity (EC_a) as a means of monitoring changes in soil inorganic N on heterogeneous morainic soils in SE Norway during two growing seasons. Nutrient Cycling in Agroecosystems 72: 213-227.

Korsaeth, A. 2005b. Relations between canopy reflectance and plant N content, above-ground biomass, yields and protein content of winter wheat and spring barley. Published in: Book of abstracts of the 5th European Conference on Precision Agriculture (ECPA), June 9-12, Uppsala, Sweden, p. 162-163.

Korsaeth, A. 2008. Dependence of Soil Apparent Electrical Conductivity (EC_a) upon Soil Texture and Ignition Loss at Various Depths in Two Morainic Loam Soils in Southeast Norway. In: Handbook of Agricultural Geophysics (Eds. Barry J. Allred, Jeffrey J. Daniels, and M. Reza Ehsani), p. 217-223. CRC Press, Taylor & Francis Group, New York.

Korsaeth, A., Ørka, H.O., 2007. Classification of crops using an airborne hyper-spectral imager. Poster papers of the 6th European Conference on Precision Agriculture (ECPA), June 3-6, Skiathos, Greece, p. 1-6 (on CD).

Korsaeth, A., Riley, H., Kværnø, S.H., Vestgarden, L.S., 2008. Relations between a Commercial Soil Survey Map Based on Soil Apparent Electrical Conductivity (EC_a) and Measured Soil Properties on a Morainic Soil in Southeast Norway. In: Handbook of Agricultural Geophysics (Eds. Barry J. Allred, Jeffrey J. Daniels, and M. Reza Ehsani), p. 225-231. CRC Press, Taylor & Francis Group, New York.

Øvergaard, S.I, Isaksson, T., Kvaal, K., Korsaeth, A. 2010. Comparisons of two hand-held, multispectral field radiometers and a hyperspectral airborne imager in terms of predicting spring wheat grain yield and quality by means of PPLS regression. Journal of Near Infrared Spectroscopy. In press.

Application of EM sensors in archaeology: EM survey at the manor Nr. Vosborg, Denmark

Mogens H[1]. Greve, Kristian Dalsgaard, Helle Henningsen and Jan Kock,*

1) Faculty of Agricultural Science, Aarhus University. Denmark

** Correpsonding author, E-mail: MogenH.Greve@agrsci.dk*

In Denmark EM survey has been widely used in agriculture since 1999 and relative large areas has been mapped by the Aarhus university and Danish agricultural advisory service on a commercial basis and in relation to research. The experience with archaeological survey in Denmark has been done by our institute the last 5 years.

The importance of EM instruments, both the Geonics EM38 and the DULEM 1s and 21s used in our surveys, lies in its availability, its data collecting speed, and its particular geophysical sensitivity. It also can be used to measure two types of information, earth conductivity (measured in mS/m or millisiemens/meter) and magnetic susceptibility (measured in ppt or parts per thousand) both measurement showed very use full in this survey.

Because of its potential speed of ground coverage and its particular sensitivity, it may be used to cover wide areas quite rapidly. This is important in surveying large archaeological features like earthworks and buried buildings, roads or other large line elements in the landscape quite often, pattern recognition depends upon getting a large-scale view of the anomaly.

In cooperation with archaeologists from Aarhus University and the local museum of Holstebro, a survey around the mid 16th century ruin site of the castle of Sdr. Vosborg in the most western part of Denmark was initiated. The results were convincing and gave good guide lines to the archeologists on "were to dig". Since the method is very fast, an extended area around this castle site was mapped, and a couple of hundred meters from the site a large anomaly was detected along with small pieces of tile in the plough layer.

A large scale archaeological excavation was accomplished on the anomaly, which proved to be the remains of the imposing castle of Vosborg from the mid 14th century. Until these surveys, this aristocratic castle was only known from scarce written sources. The castle consisted of two artificial banks made by turf and sand in a delta area. On the main bank were the ruins of an unusually large brickbuilt house. The castle had been totally destroyed by a fierce storm surge in the late 16th century.

In this survey the EM sensors (in this case the DUALEM 1s) has proven very useful for archaeological surveys, but it also showed us the importance of thorough pretreatment of the survey data. It is very valuable to ad a very accurate RTK-GPS in order to be able to utilize the elevation information from the GPS since a detailed DEM gives very important supplementary information.

A Mole turning about soils: application of gamma ray soil sensor systems

Eddie Loonstra

The Soil Company, Leonard Springerlaan 9, 9727 KB Groningen, The Netherlands.

Phone: +31 505773240, Fax: +31 505772534, E-mail: loonstra@soilcompany.com

Introduction

The use of proximal soil sensors for soil mapping is gradually increasing. Whereas tools as EM can be considered rather common used, gamma ray soil sensors are relatively new in soil science. Gamma ray sensors have a history in geology (Grasty et al., 1985) and the mining industry, especially in borehole conditions. With the development of mobile proximal gamma ray sensor systems in the 1990s it is also used for mapping soil properties (Viscarra Rossel et al., 2007; van Egmond et al., 2008). These passive systems are capable of measuring the gamma ray energy that is emitted by soil and rocks on-the-go. Typically, a gamma ray sensor measures the energy spectrum from 0 to 3000 keV of the radiation that reaches the surface. In general, 95% of the measured radiation originates from the top 30-40 cm of the soil.

Technology

A gamma sensor system consists of different components, a crystal that captures the radiation, a photomultiplier and a multi-channel analyser. The crystals are manufactured from different materials, including NaI, CsI and BGO crystals, each which their own merits (Hendriks, 2001). Primary components of the energy spectrum are the decay products of ^{232}Th, ^{238}U, ^{40}K, ^{137}Cs. The first three elements are natural, Cesium is man-made and can be measured in Europe for instance as a result of the Chernobyl accident.

The Mole is gamma ray soil sensor system that applies a Full Spectrum Analysis method (FSA) to get information on nuclide activity. FSA performs a Chi square optimisation on the entire spectrum using a set of standard spectra. A standard spectrum is the full spectrum derived when measuring 1 Bq/kg of a nuclide. This yields the quantity of energy emitted by the separate nuclides in Bq/kg (Hendriks, 2001). Mole sensors have been applied since 2001 and this paper will deal with the major applications of this soil sensor system.

Applications

The Mole technology was initially developed for purposes of precision agriculture. Therefore the nuclide information from soils needed to be correlated to relevant soil properties. It turned out that strong correlations exists between the nuclei and physical soil properties such as clay- and sand content, grain size and organic matter and the more stable soil nutrients as magnesium, potassium, calcium, phosphates and pH. This statistical fingerprinting process is described in a number of studies (Loonstra, 2008; Wijngaarden, 2002). In the last 7 years Mole maps were applied in numerous precision agriculture applications such as variable liming, fertiliser application, irrigation, planting and seeding, herbicide application, et cetera.

The ability to map the variation of soil properties within a field let to several applications in agriculture apart from the intended precision agriculture applications (Loonstra, 2010). E.g. bulb growers use the maps to control the barrenness of the soil. An application that also applies for soccer pitches. In both cases management mainly focuses on keeping the organic matter content as low as possible. Related is the management of a golf course, where the mapping of physical soil properties is useful in matters of liming (pH control) and water. Another market where soil quality is an important issue is in the production of garden bushes and trees. A specific texture is often required for the production of these plants. Whereas the producer of

bushes and trees tries to manage the soil quality, the plant breeder tries to determine to what degree soil variation is of influence on plant quality. Further on, via the fingerprinting process it was found out that the habitat of certain nematodes can be determined within fields. A final agricultural soil quality application is that of price. For real estate agents top soil property maps can be a handy tool in determining the price of land.

For a number of purposes the raw Mole nuclide soil maps can be helpful in the decision making process. They are used directly after the construction of new sport pitches to see if the variation of the soil is in line with regulations. The nuclide maps are also useful in finding soil abnormalities or disturbances. This is for instance the case at dump spots, old brooks or garbage locations, archaeological sites or deposits of dredging. The latter can be an important feature in the search for contamination sites. Examples of direct correlation between radioactive nuclides and pollution, e.g. heavy minerals, is scarce, but some positive cases were reported (M. Söderström, 2008; van der Graaf, 2007).

Recently, gamma ray soil sensors are applied in a scientific context. In the EU-funded project iSOIL several soil institutes look at the merits of this technology for digital soil mapping. In Australia the governmental institute CSIRO does the same. Mole technology is also applied by Russian scientists in order to find out what the current degree of ^{137}Cs contamination is in fields that were hit by the Tsjernobyl disaster.

Conclusion

In this paper several examples of the usefulness of high resolution soil maps from Gamma ray soil sensors like the Mole was highlighted. The nuclei variation maps as well as the composed soil properties have proven to be of assistance in various soil related issues and decisions. Gamma ray soil sensors can become an important tool for anyone that is concerned with top soil. Further applications are expected in wine production and issues of erosion and water management, almost certain in combination with different technology.

References

Van Egmond FM, Loonstra EH, Limburg J (2008) Gamma ray sensor for topsoil mapping the Mole 1st Global Workshop on High Resolution Digital Soil Sensing and Mapping, Sydney

Van der Graaf ER, Koomans RL, Limburg J, de Vries K (2007) In situ radiometric mapping as a proxy of sediment contamination: Assessment of the underlying geochemical and -physical principles. Applied Radiation and Isotopes 65(5), 619-633.

Grasty RL, Glynn JE, Grant JA (1985) The analysis of multi-channel airborne gamma-ray spectra. Geophysics 50, 2611-2620.

Hendriks PHGM, Limburg J, de Meijer RJ (2001) Full-spectrum analysis of natural γ-ray spectra. Journal of Environmental Radioactivity 53, 365-380.

Loonstra EH, A Mole collecting fingerprints: a gamma ray sensor for measuring physical properties of top soil. IAMFE 2008, Aarhus. Denmark.

Loonstra EH, Precision farming results based on the Mole: "A gamma ray soil sensor system for high resolution digital soil maps". AgEng 2010, Clermont Ferrand, France.

Söderström M, Eriksson J, Gamma ray sensing for cadmium risk assessment in agricultural soil and grain: a case study in southern Sweden. HRDSSM 2008. Sydney, Australia.

Viscarra Rossel RA, Taylor HJ, McBratney AB (2007) Multivariate calibration of hyperspectral γ-ray energy spectra for proximal soil sensing. European Journal of Soil Science 58, 343-353.

Wijngaarden van, M., Venema, L.B., De Meijer, R.J., Zwolsman, J.J.G., Van Os., B. and Gieske, J.M.J., 2002. Radiometric sand-mud characterization in the Rhine-Meuse estuary Part A: Fingerprinting. Geomorphology, 43: 82-101.

Application of sensor technology as a tool in an improved crop quality certification system – a study on cadmium risk assessment

SöderströmM[*1] and Eriksson, J[2]*

SLU, Swedish University of Agricultural Sciences

1) Department of Soil and Environment, Precision agriculture and pedometrics, P.O. Box 234, SE-532 23 Skara, Sweden.

2) *Department of Soil and Environment, Biogeochemistry, P.O. Box 7014, SE-750 07 Uppsala, Sweden.*

**) corresponding author, Phone: +46(0)51167244, E-mail: mats.soderstrom@mark.slu.se*

Background

A certification system, "Swedish Seal of Quality" (Sigill), is in place for quality and environmental control in Sweden. A low Cd level in grain delivered is one criterion for certification. Currently, farmers with a soil Cd level above 0.3 mg kg^{-1} are required to analyze Cd in the crops. In some geographic areas, grain Cd often exceeds the currently permissible limit of 80 µg kg^{-1}. Through the certification systems analysis database it is possible to locate areas where high Cd levels occur, but the analyses procedure prevents a detailed analysis of the local spatial variability of Cd in crops and soil. The usefulness of national soil and crop surveys (e.g. Eriksson et al., 2010) is limited in depicting areas with high or low Cd contents in crop or soil, more than in very general terms. The sampling density is often low and a sample will represent a very large area.

Frequently, high soil Cd areas are often found in areas where the parent bedrock at least partly is alum shale (Eriksson et al., 1995). The content of uranium (U) in the soil is also normally related to occurrences of this parent material. Since the 1960's, U has been mapped by airborne gamma-ray measurements of the ^{238}U isotope by the Swedish Geological Survey (SGU), and recently available comparable equipment mounted on a motor vehicle can be used for very detailed gamma-ray scanning. The natural emission of gamma-rays from the rock outcrops and soil reflects both the type of bedrock and the bedrock weathering and the processes of soil development (e.g. IAEA, 2003; Wilford & Minty, 2007).

In this study, the objective was to test whether airborne and proximal gamma-ray measurements can be used for detailed risk assessment for Cd in agricultural soil in an area in eastern Sweden (Östergötland) that is rich in alum shale. Results from this project have been published in Söderström & Eriksson (2010).

Material and methods

Data from airborne gamma-ray spectrometry measurements in the SGU (Swedish Geological Survey) radiometric database was used to create regional maps of the isotope ^{238}U (Figure 1). In addition, ground-based, high resolution gamma-ray sensing was carried out from a motor vehicle at four agricultural fields in the area (using *the Mole* sensor, a gamma-ray sensor for top-soil mapping developed by the University of Groningen and The Soil Company (The Soil Company, Groningen, The Netherlands)). Fifty-six samples of topsoil (0-20 cm) and fifty-nine samples of winter wheat (*Triticum aestivum*) grain were collected and analyzed for Cd. The grain sampling locations were chosen to cover areas of high and low values of ^{238}U (in 2007) from the airborne survey as well as different soil types according to the SGU soil map (in 2006).

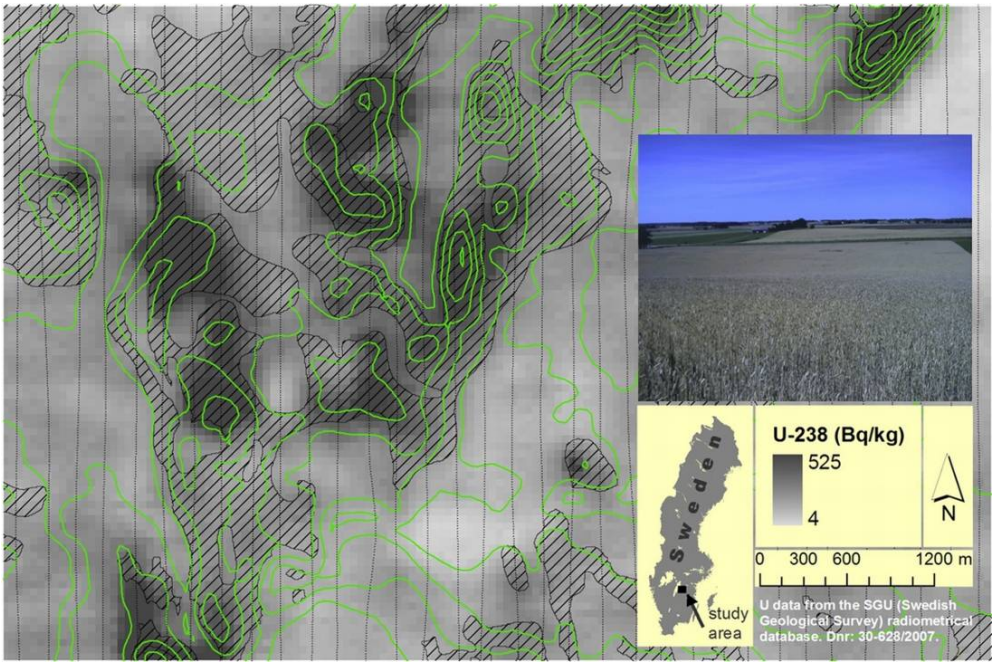

Figure 1. Interpolated values of ^{238}U from air, measured along transects with 200 m spacing (marked). In addition, areas covered by glacial till (hatched) and 5 m elevation contours are displayed. The inserted photo shows typical scenery of the area (Söderström & Eriksson, 2010).

Results

The correlation between soil Cd and the ground-based ^{238}U maps was fairly strong, but the relationship varied between the different fields or parts of a field. The airborne measurements of ^{238}U were also well correlated with soil Cd, despite the fact that latter provides a more regional overview. There was also a clear positive correlation between the airborne ^{238}U map and Cd in winter wheat grain in the 2007 samples. Cd in grain in the 2006 samples were more scattered and values were generally higher.

For the farmers connected to the *Sigill* certification system it would be valuable if some fields could be classified as low risk for Cd in grain, without the need for analysing Cd in the soil. A system of "green cards" for such areas has been suggested. In the studied area, it seems evident that the alum shale is the primary source of Cd in the soil. Given this framework, it seems reasonable to suggest that the described sensing techniques can be used for Cd risk classification of agricultural land in areas such as this. A conceptual model of how these techniques could be applied in practise is shown in Figure 2. The goal would be that farm land classified as low risk for Cd could receive a "green card" and wouldn't have to test for Cd in grain. In areas where the main source of Cd is U-rich bedrock, it should be sufficient to do this initial classification based on airborne gamma-ray sensing combined with targeted sampling of soil and crop to develop a risk classification model for the area. Bearing in mind the differences in relationship between airborne ^{238}U and Cd in winter wheat grain, the sampling for Cd in soil and crop is crucial. It is advisable that such a risk model is developed by a method that includes the uncertainty of the ^{238}U data, e.g. indicator kriging or fuzzy classification.

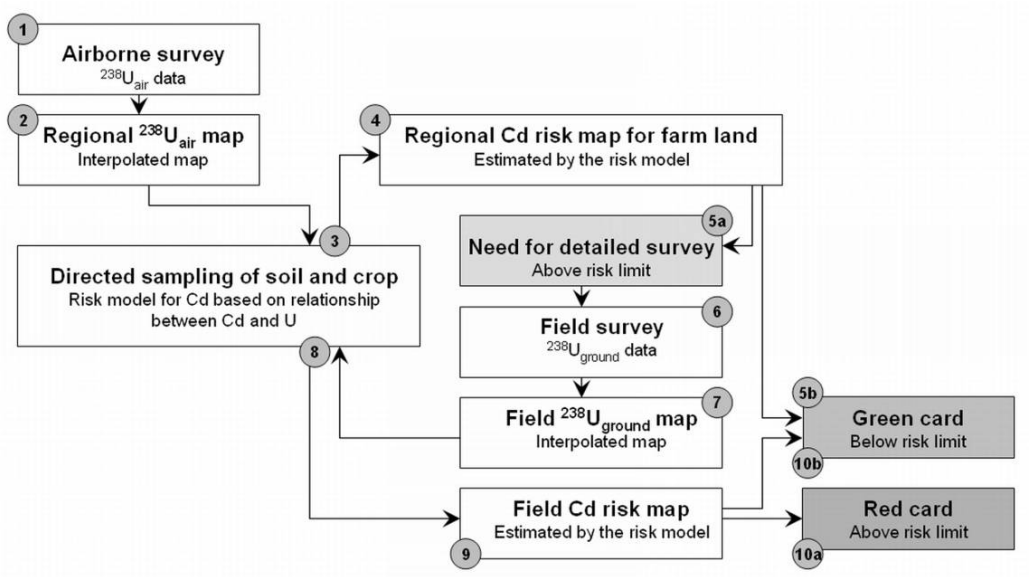

Figure 2. Suggested steps of cadmium risk classification of agricultural land based on gamma-ray sensing in areas where the main source of cadmium is bedrock rich in uranium, such as alum shale (Söderström & Eriksson, 2010).

References

Eriksson, J., Söderström, M. & Andersson, A., 1995. Cadmium contents in the plough layer of Swedish agricultural soils. Swedish Environmental Protection Agency, report 4450. Stockholm, Sweden.

Eriksson, J., Mattsson, L. & Söderström, M., 2010. Current status of Swedish arable soils and cereal crops. Data from the period 2001-2007. Swedish Environmental Protection Agency, report 6349. Stockholm, Sweden.

IAEA, 2003. Guidelines for radioelement mapping using gamma ray spectrometry data. International Atomic Energy Agency (IAEA). IAEA-TECDOC-1363. Vienna, Austria.

Söderström, M. & Eriksson, J. 2010. Gamma-ray sensing for cadmium risk assessment in agricultural soil and grain – a case study in southeastern Sweden. In: Viscarra Rossel, R. A. , McBratney, A. B. & Minasny, B. Proximal Soil Sensing. Progress in Soil Science, Vol.1, Springer, pp. 333-342.

Wilford, J. Minty, B., 2007. The use of airborne gamma-ray imagery for mapping soils and understanding landscape processes. In: Lagacherie, P., McBratney, A.B. & Voltz, M. (Eds.), Digital soil mapping – An introductory perspective. Developments in Soil Science, Volume 31. Elsevier, pp. 207-218.

Estimation of molybdenum content in topsoil using gamma ray sensing

Ulf Axelson[1], Henrik Stadig[1], Mats Söderström[2] and Anders Jonsson[2]*

1) Rural Economy and Agricultural Society of Skaraborg

2) Precision Agriculture & Pedometrics, Dept. Soil and Environment, SLU

**) corresponding author, Phone: +4651124837, fax +4651118631, E-mail Ulf.Axelson@hush.se*

Introduction

High levels of molybdenum (Mo) in forage can cause secondary copper deficiency in ruminants (Gardner et. al., 2003). Extremely low levels of Mo can have the opposite effect, i.e. copper toxicity. A high level of Mo in soil increases the likelihood of high Mo uptake in forage crops (Majak et. al., 2004). In order to avoid the problem of secondary copper deficiency in ruminants, it is important to identify farm fields with high levels of Mo in the soil. The Mo content generally depends on the parent mineral of the soil. The mineral composition and texture can undergo considerable variations within short distances, i.e. within fields. It is therefore important for farmers to be able to identify fields or parts of fields with high Mo levels if they are to manage their forage production in ways that reduce the risk of copper deficiency. Detailed knowledge of variations in soil Mo is also important e.g. in determining the location of field trials on Mo uptake by forage crops.

Therefore a study was carried out to test the possibility of using a gamma ray sensor in the field to estimate variations in Mo content in the topsoil.

Materials and Methods

A transect along the slopes of Ålleberg mountains, south-west Sweden, was scanned with the Mole instrument (Soil Company, Groningen, the Netherlands), a gamma ray sensor that was mounted on a 4WD quad-bike. Scanning was also carried out at two farms close to Ålleberg. Thirteen reference Mo soil samples were obtained at locations selected in order to cover the variation recorded by the sensor.

Results and Discussion

Parts of the Ålleberg mountains consist of alum shale, a type of rock that is rich in Mo. There were considerable variations in Mo concentration along the transect. The correlation between soil Mo and gamma ray ^{238}U was found to be very high (r^2=0.90) (Figure 1).

When data from the two farms close to Ålleberg were included, the correlation was somewhat lower (r^2=0.73). The relationship between soil Mo and ^{238}U in two soils with a high content of organic matter (13.6% and 46,6%) deviated from that in other soils and these soils were therefore excluded from estimation of the determination coefficient.

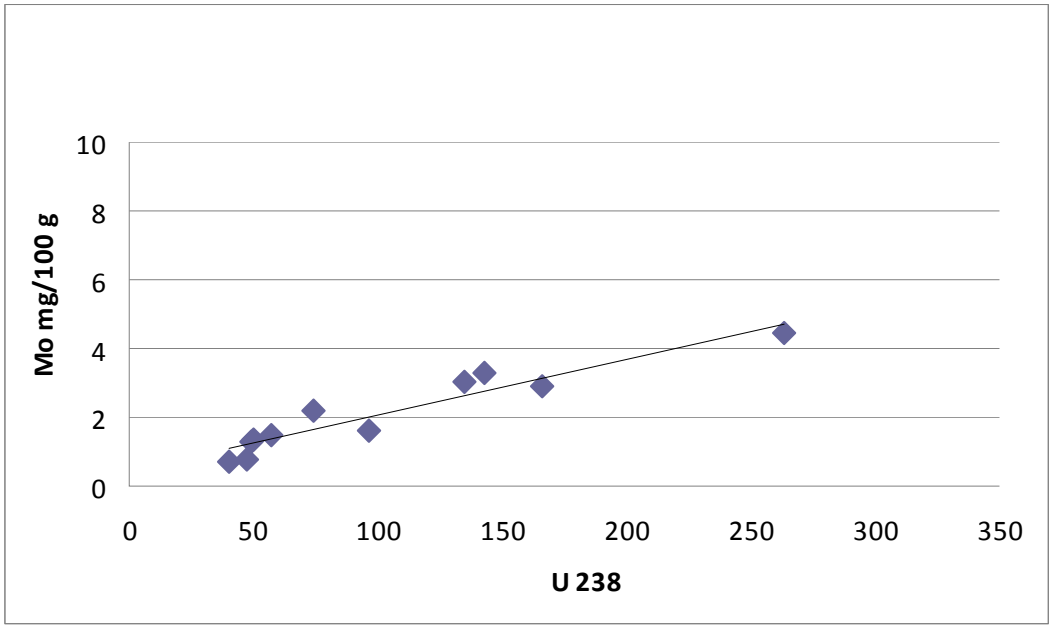

Figure 1. Correlation between ^{238}U and Mo (mg kg^{-1}) in topsoil along the Ålleberg transect.

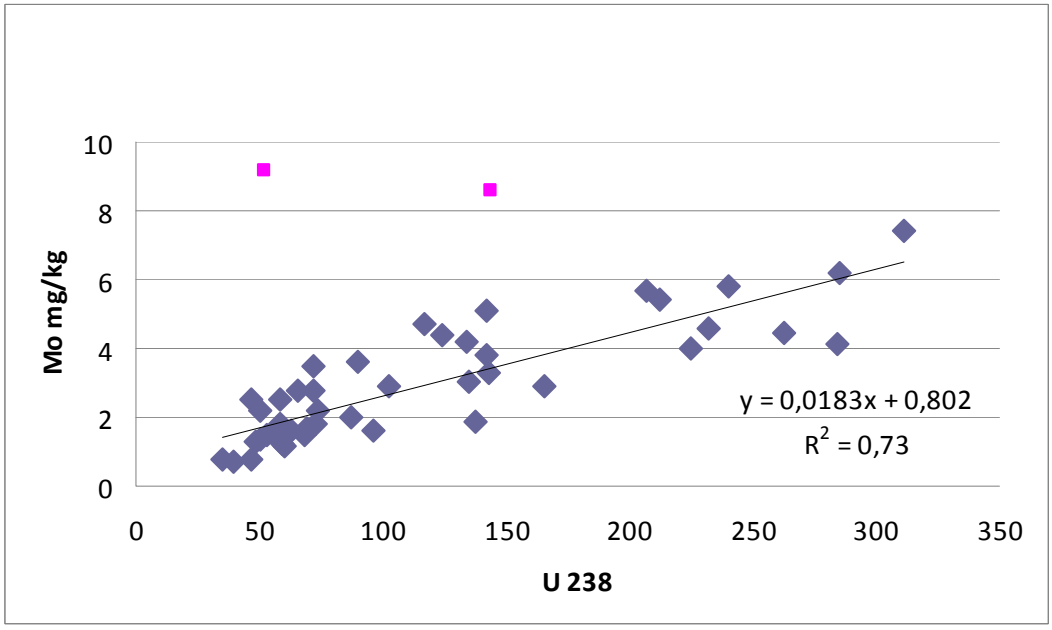

Figure 2. Correlation between ^{238}U and Mo (mg $kg^{-1)}$ for topsoil along the Ålleberg transect and topsoils at two neighbouring farms. Two soils with high organic matter content were treated as outliers and were excluded.

Conclusions

Gamma ray sensing can be used for identification of fields or parts of fields with high levels of Mo in the topsoil. The technique is considered suitable for determining appropriate sites for field trials in a continuation of this project, where we will test the effects of addition of sulphur on uptake of Mo in plants.

References

Gardner, W.C., Broersma, K., Popp, J. D., Mir. Z., Mir, P.S. and Buckley, W.T., 2003. Copper and health status of cattle grazing high-molybdenum forage from reclaimed mine tailing site. Canadian Journal of Animal Science 83 (3), 479-485.

Majak, W., Steinke, D. , McGillivray, J. and Lysyk, T., 2004. Clinical signs in cattle grazing high molybdenum forage, Journal of Range Management 57(3), 269-274.

Canopy sensors; Potentials and limitations

Anton Thomsen

Faculty of Agricultural Sciences, University of Aarhus, Denmark

E-mail: Anton.Thomsen@agrsci.dk

Spectral canopy sensors for application to precision agriculture have been commercially available for more than 10 years. The most recently developed sensors are active and can be used independent of solar radiation. Also the user friendliness and ease of integration with tractor computers and implement controllers has been greatly improved (Topcon CropSpec plant nutrition sensor developed in cooperation with Yara International). The Cropspec and similar sensors are typically used for redistributing a given amount of nitrogen (N) fertilizer within a field based on spectral measurements alone. Measurements provide a relative measure of crop N status and the absolute N status and need for additional N fertilizer in kg/ha is not predicted in typical applications. Also variation in crop density cannot be predicted independently and areas with low plant densities tend to be over fertilized. Because of the limited ability to predict the absolute N status and demand the application of the commercially available sensor has been shown to have a very limited effect.

The experimental canopy sensor, MobilLas, has been developed for variable rate fertilization, plant protection, irrigation, and other applications related to precision agriculture. Sensor development has been based on extensive experimentation including research plots and entire fields. The MobilLas sensor includes two instruments measuring canopy spectral reflection and structure (height, density, leaf area, leaf angle distribution) respectively. The current prototype includes active sensors (radiometer and laser range finder). By combining measurements canopy N status (amount of nitrogen taken up by the crop) and the need for further N application to reach a target development and yield can be predicted. The current sensor was tested during 2009 in a field experiment including winter wheat. The results demonstrate the high quality of the individual measurements and the robustness of the sensor for precision N fertilization. Because of the combination of spectral and structural canopy measurements - a unique feature of MobilLas – N status is calculated without the need for any plant related input (e.g. development stage) from the user. The 2009 results demonstrate that the sensor predicted N status and the need for further fertilization is nearly constant for weeks prior to the final dressing and the sensor can be used in offline mode to map the N status of a large number of fields. The application to plant protection, irrigation scheduling etc. awaits further development of algorithms and management models before ready for field application. Compared to single instrument canopy sensors the double sensor approach involves more complicated and expensive electronics and the development of crop specific fertilization algorithms etc.

Measurements made by the MobilLas sensor are used to illustrate the use of canopy sensors for optimizing N fertilization.

The use of Yara N-Sensor in Sweden

Knud Nissen

Lantmännen, Östra Hamnen, 531 87 Lidköping, Sweden,

Phone: +46-510-888 19, E-mail: knud.nissen@lantmannen.com

Introduction

POS (Precision farming of Sweden) together with Lantmännen and Yara have since 1998 been working with improving and developing new applications in the Yara N-Sensor for Scandinavian conditions. Today (2010) there are 80 N-sensors in Sweden and they spread approximately 50 000 ha. In average each sensor spreads between 600-800 hectares per year. In 2010 around 900 Yara N-Sensors have been used for variable N application on practical farms in Europe.

Nitrogen application with the Yara N-Sensor

In the beginning it was mostly contractors who had Yara N-Sensors, but today most of the sensors are owned by farmers using them on their own farms. The sensors are mainly used to apply the last fertilization (the third dressing if it is bread wheat, and the second dressing if it is feed wheat). Today it is also common to use it in the main fertilization of winter rape and winter wheat. Now that the sensor is on the farm there are also many farmers who use the sensor to apply the fertilization to various crops for example barley, oats, grass for seeds and potatoes. Historically the sensor is well known to be able to apply the nitrogen site-specifically in the second and the third dressing, especially in winter wheat (Link et al., 2002). In principle, one can use the sensor at all times to apply fertilization in any growing crops.

Agronomic calibration

Normally it is the farmer who decides the level of nitrogen application. To get the right level, the farmer should use an N-tester, his advisers and common sense. Then the Yara N-Sensor helps to distribute the fertilizer in different parts of the field. When the farmer has set a level of nitrogen, he should make an agronomic calibration in the Yara N-Sensor to get the right amount of nitrogen to the current crop.

In the Yara N-Sensor the slope of the distribution curve has a specific relationship to a given crop and growth stage that is implemented in the N-Sensor software (figure 1). The decision of the absolute level of N fertilization (the position of the curve), depends, among other things, on the cultivar and has to be made on the field. During the agronomic calibration the farmer puts a certain amount of nitrogen in relation to the N-Sensor value on the calibration area. See the example with the blue rings in figure 1. The agronomic calibration moves the distribution line forwards or backwards. The slope is fixed and depends on the growth stage and crop. The higher N-Sensor value the better N status of the crop and this means a lower N fertilizer demand.

If there are places in the field with poor crop that will not give a harvest the biomass cut-off is a threshold which indicates the poorly developed crop, if N-Sensor values are below this threshold N rates are automatically reduced in order to avoid over-fertilization. The farmer can also set the maximum and minimum N rates, although if normally it is not recommend. The result is that the desired amount will be spread in the field, in average, and the Yara N-Sensor helps to distribute the fertilizer in different parts of the field.

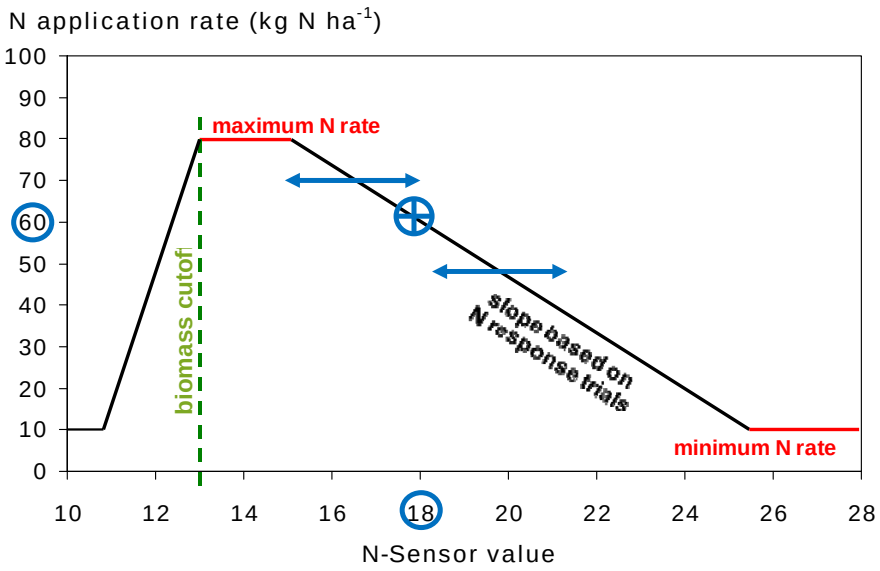

Figure 1 Conversion of reflectance measurements into fertilizer recommendations

Conclusion

With the YARA N-Sensor it is possible to detect differences in crop nitrogen nutrition status within a field and to apply N fertilizer accordingly. The farmer can determine the level of nitrogen application. Over- or under-fertilization can be avoided. This increases yield and N use efficiency. The crop stand becomes more homogeneous with more even ripening and drying. This makes the crop easier to combine and the costs are reduced.

References

Link, A., M. Panitzki, and S. Reusch. 2002. Hydro N-Sensor: Tractor-mounted remote sensing for variable nitrogen fertilization. In: Proceedings of the 6th International Conference on Precision Agriculture. July 14-17, 2002, Minneapolis. ASA-CSSA-SSSA, Madison, Wisconsin.

Reusch, S., A. Link, and J. Lammel. 2002. Tractor-mounted multispectral scanner for remote field investigation. In: Proceedings of the 6th International Conference on Precision Agriculture. July 14-17, 2002, Minneapolis. ASA-CSSA-SSSA, Madison, Wisconsin.

Wollring, J., S. Reusch, and C. Karlsson. 1998. Variable nitrogen application based on crop sensing. The Int. Fertilizer Society Proc. No 423: 3-27.

N-sensor measurements combined with model simulations to estimate variable nitrogen requirements in spring barley

*Lina Nolin[1,3,] *, Anders Larsolle[2], Bo Stenberg[1] and Mats Söderström[1]*

1) Department of Soil and Environment, Swedish University of Agricultural Sciences, Box 234, 532 23 Skara, Sweden

2) Department of Energy and Technology, Swedish University of Agricultural Sciences, Box 7032, 750 07 Uppsala, Sweden

3) Systems Biology Research Centre/Information Fusion Research Program, University of Skövde, Box 408, SE-54128 Skövde, Sweden

**) Corresponding autho, Phone: +46 500-448632, Fax: +46 500-416325, Email: lina.nolin@his.se*

Keywords: precision agriculture, nitrogen, N-sensor, Sirius model, fertiliser, variable rate application (VRA)

Introduction

The term Precision Agriculture refers to agricultural management when considering within-field spatial variability in order to improve e.g. fertiliser or pesticide use efficiency. Several methods can be used when estimating the amount of nitrogen (N) fertiliser to be added to different parts of a field. For example can estimations be based on previous yield, real-time measurements of the growing crop or model simulations of the soil and crop. The hypothesis in this study is that by combining different sources of information like historical, sensor and simulated data, the decision support for N fertilisation can be improved.

The aim of the study is to investigate and evaluate the method of combining N-sensor (Yara) measurements and simulation model (Sirius) calculations, in order to improve site-specific N fertiliser application management. The idea is to modify a previously developed simulation model for site specific N-application and yield estimates to be updated on real-time crop growth and crop N status by incorporate N-sensor measurements at the time for supplementary N application. Combining the two methods of estimating N-requirement (i.e. estimations by the N-sensor and estimations by the Sirius model) should result in a simulated crop growth that is closer to the real crop growth. This combined *sensor-model* method should thus lead to a more realistic estimation of the N need than by using one of the methods alone. In a field experiment, N fertiliser was applied at different rates in order to derive an N response curve. The estimated crop N-requirements by the N-sensor, by the model and by the combined sensor-model method respectively, will be analyzed in relation to the N response curve.

Materials and methods

Field experiments were initiated in spring 2010 at Bjertorp farm, situated in the south-west of Sweden (N 58° 15,7 E 13° 6,7). Three experiments, 20×30 m each, were allocated to different parts of the field selected for their different soil types (Figure 1). The crop was spring barley. The experiment consisted of variable nitrogen application rates divided into two fertilising occasions, summing up to a total of 0, 67, 95, 123 or 151 kg N/ha. A hand-carried N-sensor was used 4 times during one month, the first measurement was carried out in the Zadok growth stage DC14 and the last one in DC43-45. One of the N-sensor measurements was made in connection to the second fertiliser application. The plots were harvested and analysed for grain yield and plant N content (by the NIT - Near Infrared Transmittance - method). Soil samples for mineral N analyses (at 0-30, 30-60 and 60-90 cm depth) were taken in each plot at the time of sowing and harvest.

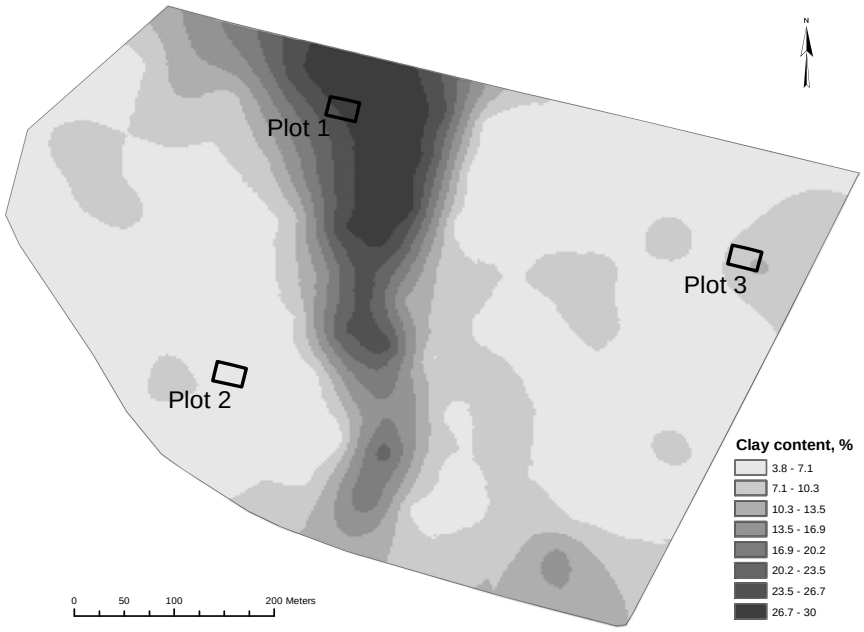

Figure 1. The field at Bjertorp farm where the three experimental plots were situated. The map shows the clay content in the topsoil layer.

The N-sensor measures the light reflectance of the crop. In the visible wavelength range (450-700 nm) the leaf chlorophyll content is recorded and in the near-infrared range (700-1000 nm) the plant biomass is recorded. The wavelength data can then be used to analyze the current plant N content and the additional N demand (Link et al., 2003).

The soil-and-crop model Sirius (Jamieson et al., 1998) simulates the crop growth and phenological stages from sowing to harvest based on soil and crop properties, weather and management input data. The model has been further developed to simulate site-specific N application and yield (Larsolle and Hanson, 2008) and it is this model version that will be used in this study.

Acknowledgement

The project was partly funded by SLF (Swedish Farmers' Foundation for Agricultural Research). Thanks to Sven Klint and Ingemar Gruvaeus at Lantmännen SW Seed AB, Bjertorp farm, for continuous information and advice of the field experiment and to Anders Grandin and the rest of the staff at Lanna field station, SLU, for management of the field experiment.

References

Jamieson P.D., Semenov M.A., Brooking I.R. and Francis G.S., 1998. Sirius: a mechanistic model of wheat response to environmental variation. Eur J Agron 8, 161-179.

Larsolle A., and Hansson P-A., 2008. Samband mellan inomfältvariation och lönsamhet vid precisionsodling. SLF (Stiftelsen Lantbruksforskning) slutrapport, VO5481106.

Link A., Panitzki M. and Reusch S., 2002. Hydro N-sensor: Tractor-mounted remote sensing for variable nitrogen fertilization. In: Robert, P.C. (Ed), Proceedings of the 6th International Conference on Precision Agriculture and Other Precision Resources Management, Minneapolis, MN, USA, 14-17 July 2002, 1465-1473.

Canopy reflectance and image analysis to determine aboveground biomass

Rikard Larsson[1], Johan Arvidsson[1] and Anders Larsolle[2].*

1) Department of Soil and Environment, 75007 Uppsala Sweden.

2) Department of Energy and Technology. 75007 Uppsala Sweden.

**) Correpsonding author, E-mail: a06rila1@stud.slu.se*

In traditional Swedish field experiments in crop production, plant development during vegetative stages is usually determined by visual assessment or by cutting the crop. Measurements of canopy reflectance as well as digital image analysis offer non-destructive and quick methods which can be used to determine crop biomass and area covered by vegetation. The objective of the work presented here was to compare measurements of canopy reflectance with measurements of aboveground plant biomass and image analysis of leaf area coverage.

Measurements were made between 16 April and 30 June in 2010 in totally 7 field experiments with soil tillage. The following crops were included: winter oilseed rape, winter wheat, spring barley, spring oilseed rape and spring wheat. A handheld Yara N-sensor equipment was used which measured reflectance in the interval 400-1000 nm. Four measurements were made in each plot of the experiments at several occasions during the spring and early summer. Two vegetation indices were used: NDVI (Normalized Difference Vegetation Index, Carlsson and Ripley, 1997) and OSAVI (Optimised Soil Adjusted Vegetation Index, Haboudane et al., 2002).

The NDVI is calculated as

$$NDVI=(R_{780}-R_{670})/(R_{780}+R_{670})$$

where R is the reflectance at a specific wavelength in nm.

OSAVI is calculated as

$$OSAVI=(1+0.16)(R_{860}-R_{670})/(R_{800}+R_{670}+0.16)$$

Until canopy closure, the crop was photographed at the same occasions as the reflectance measurements. Four pictures per plot were taken with a camera mounted on a tripod, each picture covered an area of approximately 0.22 m^2. The pictures were digitally analyzed to calculate the area covered by green leaves. The image analysis procedure consisted of two steps: 1) an automatic binarization procedure, and 2) plant coverage calculation. In the binarization step, a grey value "plant index" image was calculated from the colour information using the so called excess green index. Optimal choice of gray value threshold was then estimated using an algorithm for the automatic identification of plant and non plant peaks in the plant index grey value frequency distribution. Having the threshold, the binary image (plant or no plant) could be calculated by comparing each pixel in the plant index image with the threshold value.

At each measuring occasion, the aboveground biomass was determined. This was normally done in one of the treatments by cutting the crop in 1 m^2, followed by drying and weighing. At some occasions, 1 m^2 of the crop was cut in all plots of the experiments.

Biomass as a function of NDVI and OSAVI is shown in Fig. 1. The relationship was almost linear up to an NDVI value of around 0.8, and an OSAVI value of around 0.6. For biomasses higher than approximately 1000 g m^{-2}, there was very little change in the values of both indices. Plant coverage, as measured by image analysis, is shown in Fig. 2. For both indices, there was a curvilinear relationship and a strong correlation. The results show that canopy reflectance and image analysis are useful

methods to determine aboveground biomass. The content of nitrogen in the crop has not yet been analyzed but will also be compared with canopy reflectance measurements. The measured indices will also be compared with final crop yield in the experiments.

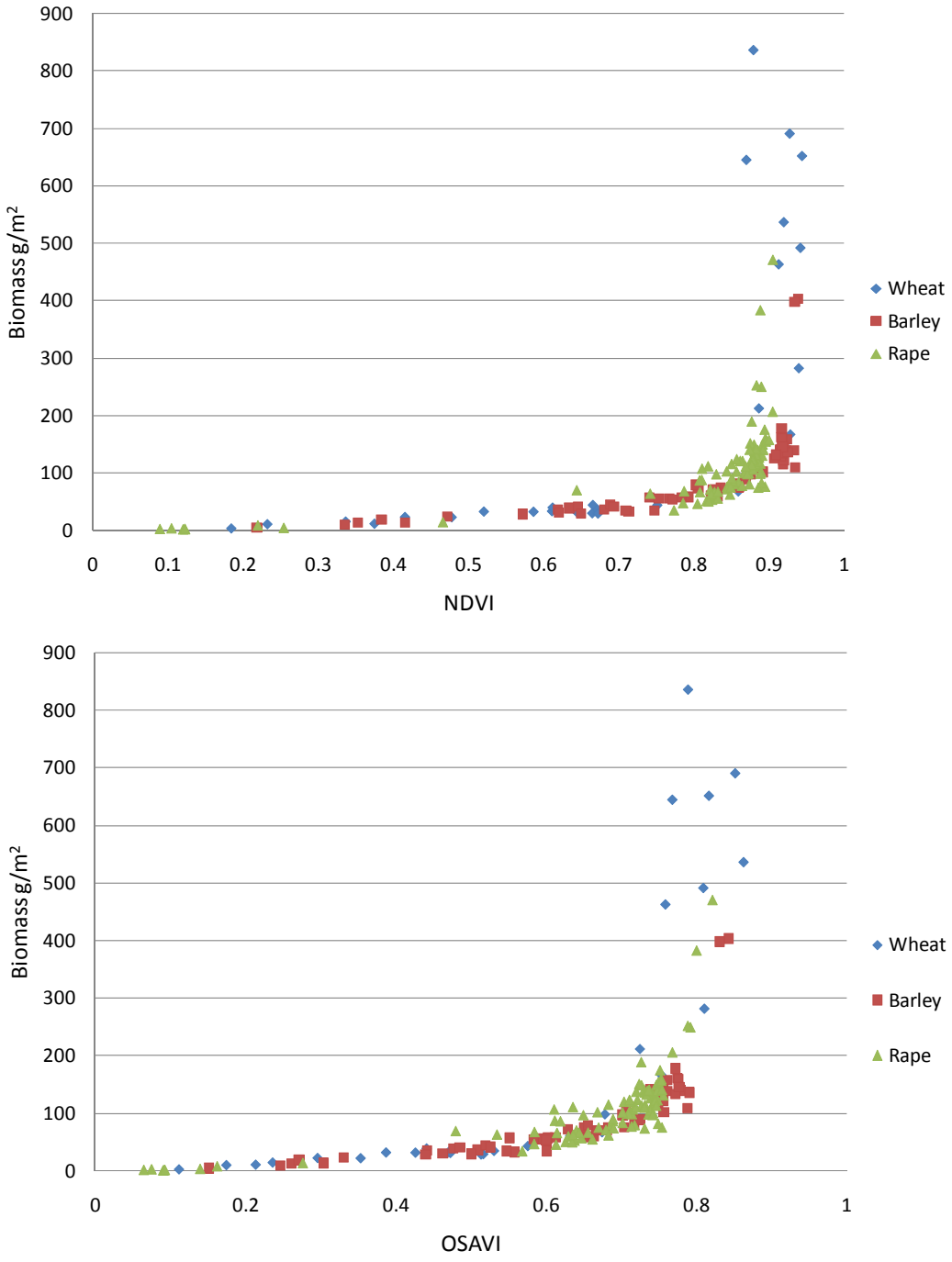

Fig. 1. Biomass as a function of NDVI and OSAVI.

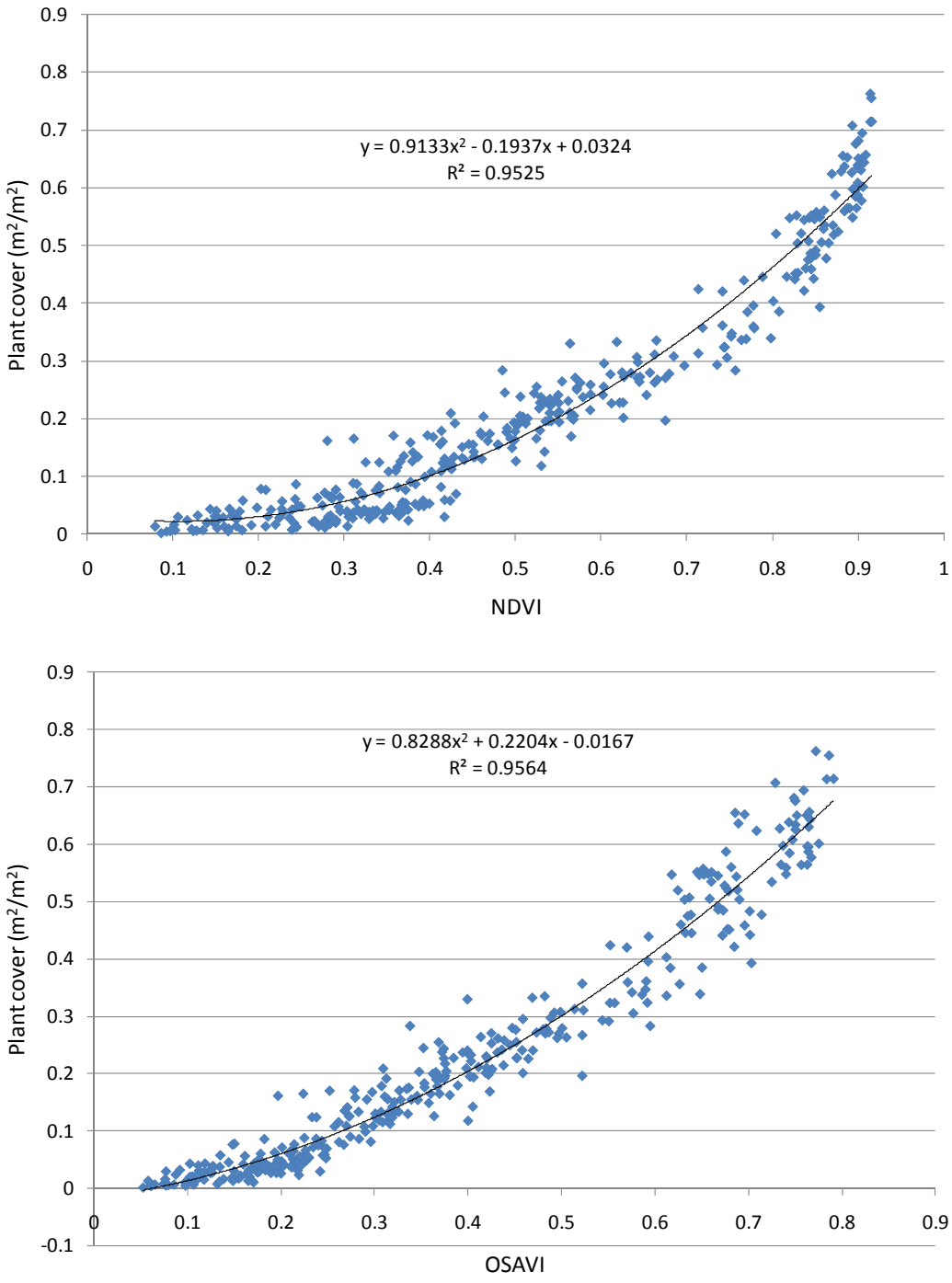

Fig. 2. Plant cover, determined from image analysis, as a function of NDVI and OSAVI.

References

Carlsson, T.N., Ripley, D.A., 1997. On the relation between NDVI, Fractional Vegetation Cover and Leaf Area Index. Remote Sensing of Environment 62, 241-252.

Haboudane, D., Miller, J.R., Tremblay, N., Zarco-Tejada, P.J., Dextraze, L., 2002. Integrated narrow-band vegetation indices for prediction of crop chlorophyll content for application to precision agriculture. Remote Sensing of Environment 81, 416-426.

Field readiness indicator

*Gareth Edwards, Ole Green and Claus Grøn Sørensen**

Department of Biosystems Engineering, University of Aarhus, Research Centre Foulum, Blichers Allé 20, DK-8830 Tjele

**) Corresponding author: Claus G. Sørensen, email: Claus.Soerensen@agrsci.dk,*

This paper presents the objectives, hypothesis and reflections of a newly started PhD project with the title: Field readiness indicator.

Introduction

A number of important factors should be investigated to construct a field readiness indicator system and to effectively predict the damaged caused to the field by initial parameters such as soil type, felid location/orientation, crop type, crop age, previous weather conditions, current weather conditions, future weather conditions, tractor size/weight, axle load, tyre width, tyre working profile, number of vehicles on the field, operational speed, etc. While the end-users are unable to affect most of these parameters, they may be able to affect those relating to the machinery used or the operational parameters. Therefore, this model can also offer advice as to the steps that may be taken to limit any damage caused.

The operation to be carried out and the soil type to be worked on are some of the most important governing factors, not only because different operations are carried out using different types of machinery, but also because different operations may require different ground conditions or moisture levels. For example, operations such as planting and fertilising may require a minimum moisture level in the soil to achieve the best results, while the soil will still have a maximum level of moisture so that no damage is caused. Therefore, the operations must be studied in-depth, along with the optimal conditions needed to determine their operational windows for minimum field damage.

The effects caused by working on a field that may be unfit as well as the effects of not working on that field at that time should also be considered as these effects can be both economical and environmental. The effect of not working on the field must then be weighed against working on the field to formulate an operation plan. The parameters that might affect not working on the field may include forecasted weather, loss in crop value, losses due to down time of machinery, extra labour, etc. While it may be problematic to work on the field at the present time, it may be justifiable to damage part of the crop rather than risk losing the total value of it.

The large number of parameters affecting both the readiness of the field and the implications of not operating on the field may lead to the construction of a very complex model. The construction of any model should be as simple as possible without losing integrity. The parameters mentioned above should therefore be investigated to establish the pre-dominate variables in the model such that any insignificant parameters can be removed. The way the model is implemented, for instance via a website, may reduce the required input parameters from an end-user such that data, e.g. weather data, may be read in automatically. Hopefully, having only a small amount of input parameters will lead to a relatively quick setup time and a more accessible product for the end-user, who may have a limited amount of time.

Research outline

When addressing this problem and constructing a model, the following steps should be taken.

- Determine the methods to classify different soil types.

- Determine the most influential parameters for soil damage. It is proposed that soil compaction is caused by pressure from machinery (a function of machinery and operation data) on soil of a certain moisture level. However, this should be verified.
- For any end-user, soil type can be considered a constant. Therefore for each soil type, the effects of different weather conditions to the moisture level within the soil should be investigated. It must be determined how far back the weather conditions must be taken into account in order to predict the current moisture level accurately.
- Expand these algorithms for one soil type such that they are applicable to other soil types. It may be necessary to construct separate algorithms for each soil type if the original algorithms cannot be adapted.
- Investigate a selection of different field operations and the machinery used in order to determine the levels of stress created by each operation on the soil and the initial conditions (i.e. soil moisture level, season, etc.) for each operation to be carried out. The modification of these operations and the options concerning machinery selection should also be investigated to allow the proposed model to be able to offer advice. This will increase the number of parameters and will add another level of control for the end-user who is able to influence the decision. As with the soil types, it may be necessary to develop separate algorithms for each operation.
- For a chosen soil type, look at the damage caused at different moisture levels with different loads or stress levels associated with different field operations.
- Construct a system based on developed algorithms to convert the parameters of the data from operations, machinery, crop, soil and weather into actionable advice and test it against independent results obtained from real-world situations.

Reflection

These parameters must be investigated and tested in a variety of different ways to assess the important interactions between them such that the overall number of parameters may be reduced. The important interactions between these parameters must also be investigated and tested in order to produce a robust system (or set of algorithms) that is able to offer advice on when the desired operation should be carried out and any precaution that may be taken to minimise any damaged caused. The system should be assessed by the accuracy of its prediction and how easy it is for an end-user to operate. It should also be assessed against any economic savings resulting from its advice or predictions in order to determine whether it is a commercially viable product.

Multisensor approach to soil mapping

Mogens H. Greve

Faculty of Agricultural Science, Aarhus University. Denmark

E-mail: MogenH.Greve@agrsci.dk

For various purposes, archeology, site specific land management and geo-techniqs the demand for cheap and detailed soil information is increasing. For decades much research has been directed towards the development and application of a variety of specialized sensors. The next logical step is off course to combine sensors that complement each other and develop increasingly sophisticated applications. The vision for myself and many other 'soil mappers' has been to install a number of great sensors on an ATW traversing the landscape and with very little effort obtain quantitative maps of a range of soil properties.

In this presentation I will focus on invasive and proximal sensors only excluding classical remote sensing techniques, and present the state of the art within the following three areas:

- Selection of sensor types for soil mapping
- Introduction of soil features / parameters that can be mapped
- Integration of complementing soil sensors.

Based on a case study made by our research group at the Aarhus University in Denmark, I will present the initial experiences with the fusion of a VIS/NIR system with soil EC and temperature with the main purposes of mapping the spatial distribution of TOC. The study field was highly variable with sandy, organic and mixed areas.

The development of new soil mapping techniques is important for the efficient management of agricultural food production while at the same time protecting the environment. The development of tools for both efficient and sustainable food production is a key issue in a world under increasing population pressure.

Sensor data fusion for topsoil clay mapping of an agricultural field

Piikki K., Söderström M., Stenberg B.*

SLU, Swedish University of Agricultural Sciences, Department of Soil and Environment, Precision agriculture and pedometrics, P.O. Box 234, SE-532 23 Skara, Sweden.

**) Corresponding author. Phone: +46(0)51167222, E-mail: kristin.piikki@mark.slu.se*

The aim of the present study was to evaluate and compare the ability of different combinations of spatial data (bulk electrical conductivity (ECa), gamma (γ) radiation, reflectance, drainage and elevation) to predict topsoil clay content of an agricultural field. The hypotheses were:

- ECa measurements from multiple occasions would perform better than one ECa measurement alone.
- ECa measurements with multiple measurement depths would perform better than one single-depth ECa measurement.
- Using the ECa and the γ radiation sensor together would improve predictions compared to using one sensor alone.
- Introducing information on spatial variation patterns by adding relevant ancillary data would improve the predictions of either sensor.

The study was performed on a 30 ha agricultural field in southwestern Sweden. Data were collected with proximal sensors for γ radiation (The Mole, The Soil Company, the Netherlands; ^{232}Th, ^{40}K, total count of decays) and ECa (EM38 Mk 2 2, Geonics Ltd., Canada; 4 depths x 1 occasion + 2 depths x 3 occasions). Reflectance data from aerial photography, elevation data collected with RTK-GPS and distances to the drainage system derived from a drainage map were also used as independent data. Multivariate prediction models (Partial Least Squares regression, PLS) of clay content were parameterized for different combinations of the independent variables, using the Unscrambler 9.8 software (Camo Software AS). Four reference samples per hectare were analyzed (n = 120) for clay content. Eighty random samples were used for calibration and the remaining 40 samples were used for validation. The predictive power of the different independent datasets was quantified by the coefficient of determination (R^2) between predicted and measured values and the root mean squared error (RMSE) of predictions.

The following results were summarized from the study.

- Predictions based on ECa data were improved by using multitemporal measurements. A likely explanation would be that information of temporally varying factors affecting ECa was added to the dataset.
- Predictions based on ECa data were somewhat improved by using measurements over multiple depths. The ECa sensor is not only affected by the topsoil but also by deeper layers of the soil. A likely explanation to the observed improvement is that the impact from deeper layers could be accounted for, by using a combination of measurements with different depth responses.
- Predictions based on ECa data were improved by adding reflectance data, while addition of drainage or elevation data only had a small effect.
- Predictions from γ radiation were found to be rather accurate (RMSE < 2% clay) and was not much improved by adding ECa or any other independent data.

Utilising proximally and remotely sensed data in soil sampling protocols

Grant Tranter[1,2] Alex McBratney[1] and Budiman Minasny[1]

1) Australian Centre for Precision Agriculture, Faculty of Agriculture, Food and Natural Resources, McMillan Building A05,The University of Sydney, Sydney, New South Wales 2006, Australia

2) Swedish University of Agricultural Sciences, Soil and Environment, Uppsala, Sweden

McBratney et al. (2003) presented the scorpan model, as a pedometric formalization of Jennys (1941) 'clorpt' model. While the 'clorpt' mnemonic is largely qualitative and explanatory, 'scorpan' models aim to provide empirical and quantitative relationships between soil and environmental factors, ultimately yielding soil spatial prediction functions. Key to the formation of such quantitative structures is the provision of spatially referenced data. It is here, that proximal and remote sensors have proved of great value, delivering spatially dense, quantitative and accountable data. Yet, while proximal sensors are excellent tools for delineating spatial variation, often is the case that some calibration is required for predictive equations of soil attributes. Generally, calibration requires physical sampling, the locations of which are determined by some sampling protocol. Within the context of DSM, the sampling protocol should aim to cover the range of the environmental covariates (e.g. proximally sensed data, elevation etc) so as to avoid extrapolation of the spatial predictive functions. This work revisits and introduces sampling protocols that utilize environmental covariates to produce efficient and effective sampling designs for digital soil mapping. A new sampling protocol is introduced, that utilizes fuzzy k-means classification of environmental covariates to obtain a predetermined number of sampling locations.

References

McBratney, A. B., Mendonca, M. L., Minasny, B. 2003. On digital soil mapping. Geoderma, 117, 3-52

Taxing Tasks in Modern Agriculture

Niels Dybro

John Deere Moline Technology Innovation Cente, One John Deere Place, Moline, IL 61265, USA

Phone: +1-309-765-387, E-mail: dybroniels@johndeere.com

Figure 1. John Deere 9630 tractor (530HP) with 48 row/30in DB120CCS planter (36.6m).

The dominating trend in modern agriculture is one of doing more with fewer people. This trend has brought about larger and more complex machines to assist the farmers in covering larger and larger land holdings. The increase in size of the farms and the machines has multiplied the task of keeping machines running and getting the field work done within the most suitable time window.

The application of monitoring systems and services has reduced the strain on the farmer in many cases, but there are still many opportunities to close the feedback control loop in modern agriculture.

The discussion will focus on: What are the types of opportunities? -and what drives adoption of new technology in these areas?

Laser Scanned Terrain Data: Potential for Merging With Other Sensor Data

Peder Klith Bøcher

Ecoinformatics & Biodiversity Group, Dept. of Biological Sciences, Aarhus University, Ny Munkegade 114, DK-8000 Århus C

Light Detection and Ranging (LiDAR) systems for terrain data acquisition have been the subject of unprecedented developments in recent years. This development is the reason as to why LiDaR is the most important geospatial data acquisition technology that has been introduced in the recent decade Shan and Toth, 2009).

Mounted on airborne platforms these systems can collect 3D data in large volumes with high accuracy. This is the main advantage of the system: it provides fine resolution digital topographic information in millimetre- to centimetre accuracy over large areas. Moreover, unlike the traditional photogrammetric methods, LiDAR collects a directly georeferenced set of 3D-points, which can be almost immediately used in basic GIS applications. However the full potentials and capabilities for LiDAR data challenges for new data processing methods that are fundamentally different from the ones used in traditional remote sensing and GIS technologies.

One main challenge is that LiDAR readily generate amounts of data, which can be tens or hundreds of gigabytes in size (Arge et al. 2003). The Danish National Elevation Model was acquired with a spatial resolution of 1.6-meters totalling almost 1.5 TB for the resulting point cloud. The mere handling these massive data on a computer represents a challenge in itself, but processing them and extracting relevant derived information poses a number of novel algorithmic challenges.

Despite this, several applications including erosion modelling, landslide risk assessment, stream mapping, and hydrologic modelling can in theory benefit from the high resolution data as the spatial resolution of these approaches the scale at which these processes take place.

These challenges are at the moment being dealt with by computer scientists that attack them with innovative I/O-efficient algorithms. These algorithms have until now increased the speed with which surface hydrological parameters for example are being computed by factors above 1000 (Danner et al., 2007). This reduction in computing time has expanded the potentials for applying surface hydrological modelling to large areas on fine resolution digital elevation models, and hence increased the opportunities for including models with much larger complexities than hitherto applied in large scale studies. The relevance for applying such methods to areas such as farming systems has therefore increased considerably.

Here we present the latest methods for computing surface hydrological parameters from terrain data and combining these with optical imagery and fine resolution soil data obtained by proximal sensors (EM-38).

For this presentation a study area near Bjerringbro in Jylland is selected which covers in large approximately 200 square kilometres (Fig. 1). The area is dominated by the river Gudenå and is generally to be characterised as an agricultural area with both patches of fields and forests as the dominating land cover.

For the purpose of investigating surface hydrological as well as soil properties a number of geospatial data were acquired:

1) Digital elevation model extracted from the National Digital Elevation Model (KMS, 2009) which is based on LiDAR data with a planar resolution of 1.6-meter and a vertical accuracy of 10-15 cm.
2) Digital orthophoto from 2006.

3) EM-38 measurements from a number of selected fields within the area.

From the digital elevation model a number of surface hydrological parameters were calculated based on the novel I/O-efficient application pipe-line "TerraStream" (Danner et al., 2007): (i) flow accumulation; (ii) Compound Topographic Index (CTI); (iii) depression analysis that maps where precipitation accumulates in cases of severe meteorological events.

The results from these computations are inspected visually as draping on top of 3D expressions of orthophotos. These illustrations brilliantly show the overall complex landscape contexts within which the hydrological patterns are to be understood.

Based on measurements conducted with an EM-38 sensor correlations computed with the hydrological parameters were performed.

Fig 1. The study area illustrated by draping orthophotos on the LiDAR based digital elevation model.

Arge, L., Chase, J. S., Halpin, P., Toma, L., Vitter, J. S., Urban, D., Wickremesinghe, R. 2003. Efficient Flow Computation on Massive Grid Terrain Data Sets. Geoinformatica Archive Volume 7, Issue 4, pp. 283-313.

Danner, A., Mølhave, Th., Agarwal, P. K:, Yi, K., Arge, L., and Mitasova, H. 2007. TerraStream: From elevation data to watershed hierarchies. Proc. ACM Sympos. on Advances in Geographic Information Systems.

Shan, J. and Toth, C. K. (ed.). 2009. Topographic Laser Ranging and Scanning: Principles and Processing. Taylor & Francis Group, Boca Raton, FL.

Mapping spatial variation in crop, willow and terrain using a small UAS

A. Rydberg[1], O. Hagner[2], P. Aronsson[3], M. Söderström[4,] and N, Adolfsson[1]

1) JTI-Swedish institute of Agricultural and Environmental Engineering, Box 7033, SE 750 07 Uppsala, Sweden. Anna.Rydberg@jti.se

2) Smartplanes , SE 910 20 Hörnefors, Sweden.

3) Swedish University of Agricultural Sciences, SE 750 07 Uppsala, Sweden

4) Swedish University of Agricultural Sciences, Box 234, SE 532 23 Skara, Sweden

Abstract

The Unmanned Aircraft System (UAS) described in this paper, SmartPlanes *SmartOne* has been approved in Sweden, Finland, Norway and Germany to operate up to 300 m altitude and within direct line-of-sight up to a distance of 800 m. It has previously been tested for precision agriculture purposes such as weed detection and mapping nitrogen and protein content variations in crops (Rydberg et al., 2007). It is currently being evaluated if spectral information from UAV can describe and quantify spatial variations of willow biomass (Rydberg et al., 2009) (Figure 1), and if advanced DTMs from UAV (Figure 2), generated by image analysis and position data, can give information about height variations on bare ground and eventually in the growing field. It is also tested whether spectral information from a UAV can identify and locate the occurrence of covered drains, as well as identify variations in soils useful for soil mapping.

The ability to accurately map within-field variability would be very useful since it enables more efficient stratified field sampling techniques to be used. If differences can be detected by means of visual interpretation it could mandate the development of more advanced automated image-analysis based tools for quantitative measurements.

Figure 1. Left: The UAS is hand launched and controlled manually to avoid obstacles. At 50 m altitude the autopilot is engaged and navigates the aircraft according to the predefined flight route. Right. Willow fields with three varieties.

The preliminary results show that it was possible to map areas with different homogeneity with high spatial precision using the orthophoto mosaic images generated with the UAS, when considering both spectral and textural information. It was also possible to differentiate between different varieties of willow using the UAS, provided that single images were used for spectral differentiation and that the stands were sufficiently large.

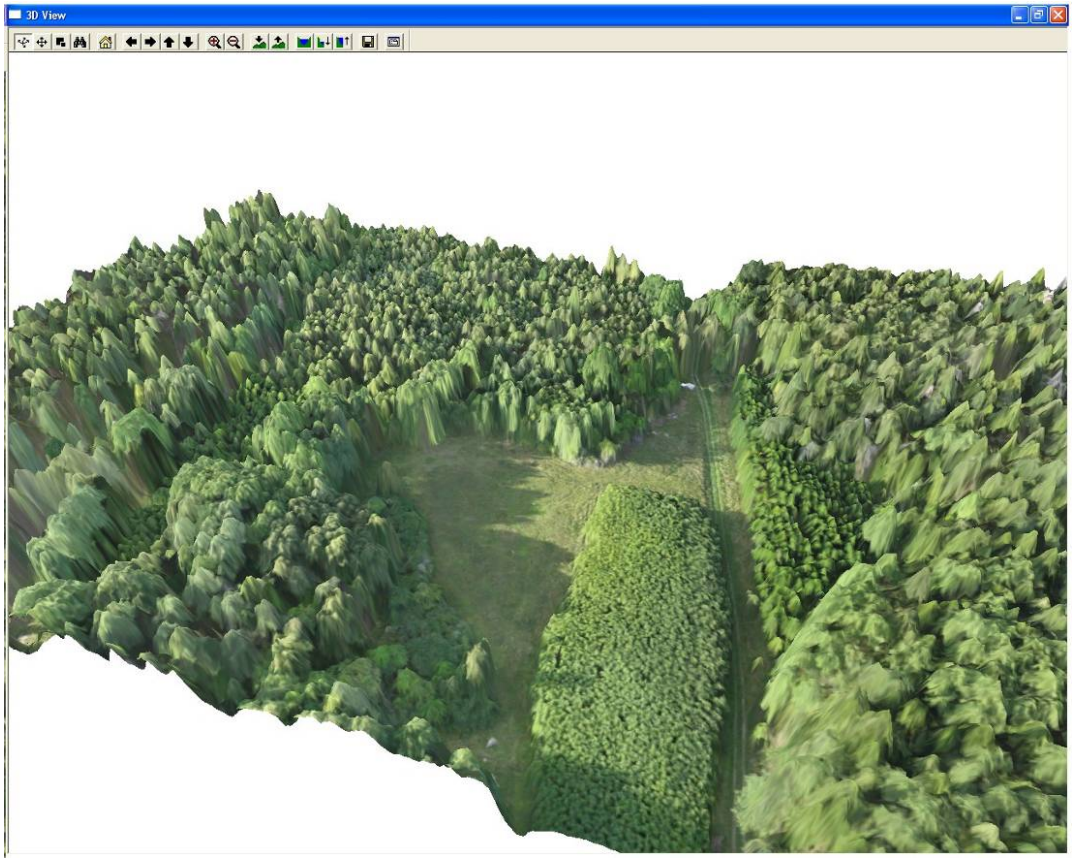

Figure 2. Digital Terrain Models (DTM) generated from the UAS.

References

Rydberg, A., Hagner, O., Söderström, M. & Börjesson, T. 2007. Field specific overview of crops using UAV (Unmanned Aerial Vehicle). In: S. Blackmore (ed.) Precision Agriculture'07. Wageningen Academic Publishers. pp. 357-364.

Rydberg, A., Hagner, O., Aronsson, P., & Söderström M. 2009. Mapping spatial variation in growing willow using small UAS. From: Henten, E.J. van, D. Goense and C. Lokhorst, 2009. Precision agriculture '09. Proceedings of the 7th European Conference on Precision Agriculture, Wageningen, the Netherlands, 6-8 July 2009, pp. 485-492.

Visible and Near infrared reflectance spectroscopy for soil analysis

Bo Stenberg

Swedish University of Agricultural Sciences (SLU), Skara, Sweden

Telephone: +46 511 67276, E-mail: bo.stenberg@mark.slu.se

Intensive and reliable soil mapping require the development of inexpensive, rapid and accurate soil analysis methods, preferably that enable measurements directly in the field. Over the last decades the use of visible-near infrared (vis-NIR) diffuse reflectance spectroscopy has been explored. The main focus has been on individual soil components, mainly clay content and soil organic carbon, SOC, or organic matter.

A soil spectrum in the vis-NIR region is generated by directing light containing all relevant wavelengths to the soil. In the visible (~400-780 nm) the relatively high energy in the radiation will mainly cause electronic excitations and in the NIR (780-2500 nm) the lower energy level will cause molecular bonds in the soil to vibrate, which involves absorption. A specific bond will absorb a specific energy quantum and this quantum corresponds to a specific wavelength (inversely to frequency). Absorptions will cause reduced reflection and the reflection relative a white reference is what is measured. Normally reflectance (R) is then transformed to apparent absorbance (A): A=log(1/R). The exact wavelength's at which absorption takes place depends also on the chemical matrix of the bond, environmental factors such as neighboring functional groups and temperature. As a soil surface is pretty far from specular not all unabsorbed energy will be reflected to the detector, but scattered. The reflection is said to be diffuse. The degree of scattering is very structure dependent. Thus, an absorption spectrum is defined by the sample's absorbing constituents and physical status.

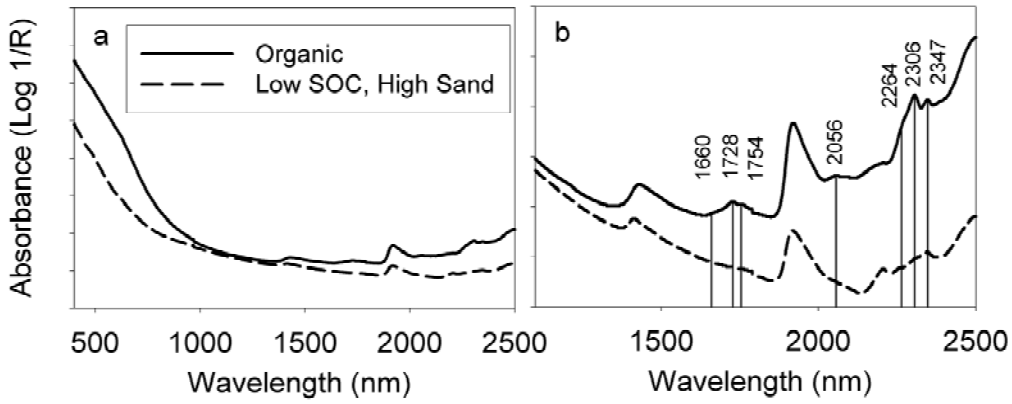

Figure 1. Two example spectra of high and low organic content. b) is an enlargement of a). Typical organic features indicated by drop-lines. After Stenberg et al. (2010).

NIR absorbance is characterized by overtones and combinations of fundamental vibrations in the mid-infrared (2500-25000 nm). This typically results in broad, superimposed and often weak vibrational modes in the NIR. Albeit absorption bands are broad and overlapping in the vis-NIR the region contains useful information about soil. In the visible mainly ferric minerals like hematite and goethite absorb. Apart from water clay minerals and organic molecules are what influence the vis-NIR spectrum the most. Soil organic matter (SOM) may have broad absorptions in the visible due to the darkness of humid acids (Fig. 1a). In the NIR overtones and

combinations of NH, CH and CO groups characterize organic matter absorptions. Bands around 1100, 1600, 1700-1800, 2000 and 2200-2400 have been identified as particularly important (Fig. 1b).

Clay mineral absorptions are mostly due to OH, H2O and CO3 overtones and combinations (Clark, 1999). Kaolinite absorb characteristically at doublets near 2200 and 1400 nm (Fig. 2). Illite and montmorillonite has single bands near 1400 and 2200 nm, and also near 1900 nm. Illite has weaker bands also near 2300 and 2400 nm. In illite and montmorillonite the 1400 and 1900 bands are due to combination vibrations of water bound in the interlayer lattices. Such water is present at larger abundance in montmorillonite and not present at all in kaolinite. Therefore absorption bands are weaker in illite and the 1900 band not at all in kaoline (Fig. 2). The 1400 absorption in kaolinite is due to overtones of OH vibrations of structural water. The 2200 absorptions are due to Al–OH plus OH combinations.

As soil organic matter, clay minerals and water are what influences NIR spectra the most. It is therefore not surprising that SOM, SOC and clay content typically are the soil parameters predicted most accurately with the most robust general calibrations (Stenberg et al. 2010). Nevertheless, several other soil attributes, such as pH, nutrient status, elements, organic matter quality, etc. are often reported to be accurately predicted. However, there is a large variation between studies with many failures reported as well. The reason is probably that these parameters don't have the strong direct relation to vibrational modes in the vis-NIR. It must therefore be assumed that these parameters are predicted through covariations to water, organics and minerals.

As an example correlation spectra to pH have been shown to be very similar to those of clay and CEC. To assume covariations to SOM and clay minerals is reasonable as both influence the buffer capacity of soil. These relationships are, however, not very robust due to for example different agricultural practice, not least liming, which will interrupt such relationships. Nevertheless, secondary calibrations like these should not be rejected, but the mechanisms behind them need to be better understood for reliable calibration strategies to be developed.

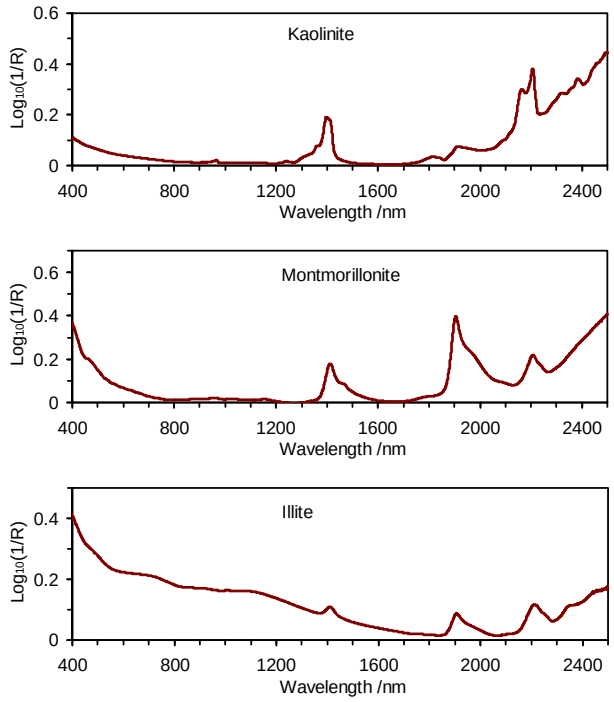

Figure 2. Example spectra of kaolinite, montmorillonite and illite minerals.

Although SOC and clay calibrations usually can be regarded as robust, the variation between prediction results is not insignificant, especially regarding the root mean squared error (RMSE). It is frequently suggested that a smaller soil variation would support better calibrations indicating a scale effect. However, reviewing a large number of published prediction results (Stenberg et al. 2010) it was found that the variation in the predicted soil property itself could explain a very large part of the variation in prediction performance (Fig. 3). For SOC, field scale calibrations could be separated, but there was only a tendency that they performed better than large scale calibrations (Fig. 3).

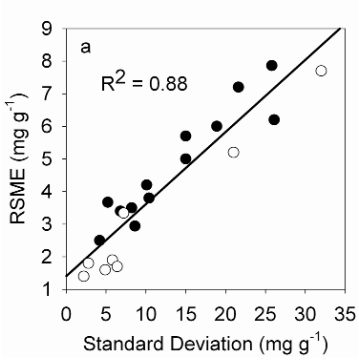

Figure 3. The RMSE of SOC calibrations as dependent of SOC variation. Filled symbols are from large scale calibrations and open symbols are from field or farm scale calibrations. From Stenberg et al. (2010).

In most work so far laboratory analysis of sieved and dried soil is the most applied strategy, but to make full potential of the rapidity and simplicity of vis-NIR spectroscopy in-field measurements should be considered. Generally this result in slightly worse predictions due to environmental and technical issues regarding sample presentation, surface conditions, reproducibility, moisture, etc. This is, however, not necessarily the case. In recent years commercial systems for on-the-go measurements with soil penetrating shanks equipped with a sapphire glass protected vis-NIR probe have been developed (Fig. 4; e.g. www.veristech.com; Christy, 2008). Veris Technologies also produce a force probe equipped with a vis-NIR sensor for point measurements while pushed down the profile. Such technology is valuable as there are few sensors that are able to give soil information from well defined depths. Another strategy is to take out an intact soil core and measure the core surface in field or in the lab, or to insert a measuring head down a pre drilled hole and measure the inner surface of the hole (Fig. 5). Such probe is being commercialized according prototype described by Ben-Dor et al. (2008).

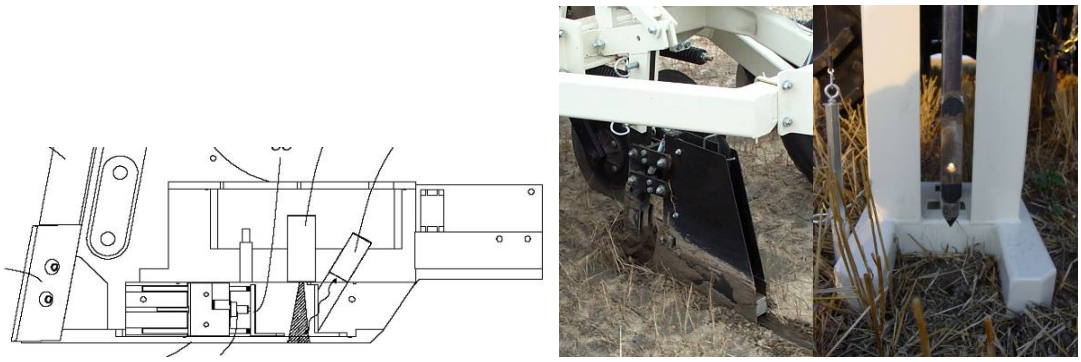

Figure 4. Veris vis-NIR shank (left end middle) and profiler probe (right).

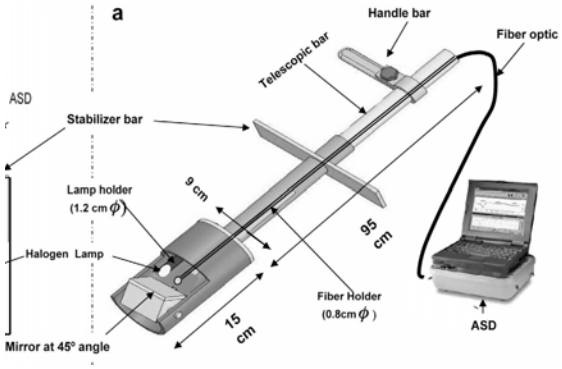

Figure 5. A sketch describing all parts of the in-soil 3S-HeD probe and the connection between the spectrometer device and the inner fore-optics. From Ben-Dor (2008)

Although variable soil moisture content and the potential weakening of soil features close to water bands broadening as water levels increase are problems often experienced the opposite has also been reported with the statistical differences between dry and field moist soils mainly found in restricted regions (1300-1600 and 1850-2100) (Viscarra Rossel et al., 2009). Different conclusions regarding this probably have to do with how moist soils are and how large the variation in the data set is. Potentially larger prediction errors need to be put in relation to what may be gained by a denser sampling made feasible by in-field measurements.

References

Ben-Dor, E., Heller, D. and Chudnovsky, A., 2008. A novel method of classifying soil profiles in the field using optical means. Soil Science Society of America Journal, 72(4): 1113-1123.

Christy, C.D., 2008. Real-time measurement of soil attributes using on-the-go near infrared reflectance spectroscopy. Computers and Electronics in Agriculture, 61(1): 10-19.

Clark, R.N., 1999. Spectroscopy of rocks and minerals and principles of spectroscopy. In: A.N. Rencz (Editor), Remote sensing for the earth sciences. Manual of remote sensing. John Wiley & Sons, Chichester, UK, pp. 3-58.

Stenberg, B., Viscarra Rossel, R.A., Mouazen, A.M. and Wetterlind, J., 2010. Visible and Near Infrared Spectroscopy in Soil Science. In: L.S. Donald (Editor), Advances in Agronomy. Academic Press, pp. 163-215.

Viscarra Rossel, R.A., Cattle, S.R., Ortega, A. and Fouad, Y., 2009. In situ measurements of soil colour, mineral composition and clay content by vis-NIR spectroscopy. Geoderma, 150: 253-266.

Evaluation of Ground Penetration Radar (GPR) for characterization of silage stack compaction

Ole Green[1], Johanne Lindstrøm[1], Rasmus Nyholm Jørgensen[2] and Claus Grøn Sørensen[1]*

1) Department of Biosystems Engineering, University of Aarhus

2) Institute of Chemical Engineering, Biotechnology and Environmental Technology, University of Southern Denmark

**) Corresponding author: Ole Green, email:Ole.Green@agrsci.au.dk, Research Centre Foulum, Blichers Allé 20, DK-8830 Tjele*

Introduction

The compaction process in a silage stack is a key process in the overall silage production as it relates to obtaining an optimal quality of the feeding silage (Williams et al., 1997, Shao et al. 2005). Also, the costs of the silage production are affected by the silage compaction. The basic principles of the compaction procedure have been known for many years (Buckmaster et al., 1990) and several analyses have been carried out to describe how the resulting silage density is affected by a number of factors. Muck et al. (2004) and Savoie et al. (2004) described how the silage density is dependent on the compaction methods and Muck & Holmes (2000), Bernier-Roy et al. (2001) and Muck & Holmes (2004) analyzed and found a significant influence from different storage methods.

Neal (2004) reports that geologists and soil scientists have used ground penetrating radar (GPR) as a method in sedimentology for many years. The GPR system functions by sending a high frequency electric impulse into the soil and measuring the reflectance time (Daniels et al., 1988). In terms of specific usage, the method has been used for characterizing soil structure, compaction and type (Petersen et al. 2005), determining water contents (Lunt et al. 2005, Doolittle et al., 2006) and localizing objects in the soil (Freeland et.al., 1998). Also, GPR has been used in agriculture as an on-line sensor in precision agriculture applications (Adamchuk et al., 2004).

The structural composition of silage has many similarities with a humus soil. Hence, the idea and objective of the presented pilot experiment were to evaluate a GPR-system for the characterization of silage stack compaction.

Results

Five profiles from a silage stack were characterized with a GPR-system and with a CP as a reference method. The profile that was located 12.5 meters from the end wall of the silage stack showed significant similarities regarding the illustrated structure of the top of the silage stack. Both of the measuring methods showed that the centre bottom of the measured area has a higher material density, and when comparing the results, the phase shifts in the GPR measurements to fit with the areas in the CP measurement where there is a distinct higher PR.

The measurements revealed that the centre of the stack is more compact in the sub part of the stack compared to the top-layers, and this is in agreement with studies made by D'Amours & Savoie (2004) which showed the same density distribution. Along the walls of the silage stack and within a distance of 1 m from the wall, the density is also lower. D'Amours & Savoie (2005) reported a similar density distribution in a silage stack confined to a concrete silo.

Based on experiences with GPR measurements, the penetration depths were estimated to a maximum range from 0.60 to 0.80 m, which is similar to the measuring depth with the CP. The reduced penetration depths are possibly caused by

high water content combined with a high salinity, while salt in the silage water increases the conductivity of the material.

In order to acquire additional knowledge about the factors affecting the radar penetration depths, it would be relevant to carry out experiments as a way to measure the dielectric resistance of various silage types. Also, measurements of the water contents and density as a function of depths may reveal how changes in these parameters would affect the radar waves.

The visual data interpretation of the two methods has shown that a GPR scan of the top layer of a silage stack is likely to give the same information as a measurement made with a high resolution penetration measure, but the advantage of the former is that the time required to perform a radar scan is substantially reduced.

References

Adamchuk, V.I., Hummel, J.W., Morgan, M.T. & Upadhyaya, S.K. (2004): On-the-go soil sensors for precision agriculture. Computers and Electronics in Agriculture, vol. 44 (2004) p. 71-91

Buckmaster, D.R., C.A. Rotz and J.R. Black. 1990. Value of alfalfa losses on dairy farms. Trans. of the ASAE. 33(2):351-360

Bernier-Roy, Tremblay, Pormerleau & Savoie (2001): Compaction and Density of Forage in Bunker Silos, ASAE meeting presentation, nr. 11089, 2001

Daniels, J.J., Grumman, D.L. & Vendi, M.A. (1997): Coincident Antenna Three-Dimensional GPR, JEEG, Vol 2, issue 1, March 1997, p 1 - 9.

Daniels, D.J., Gunton, D.J. & Scott, H.F. (1988): Introduction to subsurface radar, IEE Proceedings, Vol 135, Pt.F., No. 4, August 1988

D'Amours, L. & Savoie (2004): Density profile of corn silage in bunker silos, ASAE meeting presentation, nr. 41136, 2004

D'amours, L. & Savoie (2005): Density profile of herbage silage in bunker silos, ASAE meeting presentation, nr. 51051, 2005

Doolittle, J.A., Jenkinson, B., Hopkins, D., Ulmer, M. & Tuttle, W. (2006): Hydropedological investigations with ground-penetrating radar (GPR): Estimating water-table depths and local ground-water flow pattern in areas of coarse-textured soils. Geoderma, vol. 131 (2006) p. 317-329

Freeland, R.S., Yoder, R.E. & Ammons, J.T. (1998): Mapping shallow underground features that influence site-specific agricultural production. Journal of Applied Geophysics, vol. 40 (1998) p. 19-27

Lunt, I.A., Hubbard, S.S. & Rubin, Y. (2005): Soil moisture content estimation using ground-penetrating radar reflection data. Journal of Hydrology, vol. 307 (2005) 254-269

Muck & Holmes (2000): Factors Affecting Bunker Silo Densities, Am. Soc. Agr. Eng., year 2000, vol. 16(6), p. 613-619

Muck & Holmes (2004): Bag Silo Densities and Losses, ASAE meeting presentation, nr. 41141, 2004

Muck, Savoie & Holmes (2004): Laboratory Assessment of Bunker Silo Density Part I: Alfalfa and Grass, Am. Soc. Agr. Eng., year 2004, vol. 20(2), p. 157-164

Neal, A. (2004): Ground-penetrating radar and its use in sedimentology. Earth-Science Reviews, vol. 66 (2004) p. 261-330

Petersen, H., Fleige, H., Rabbel, W. & Horn, R. 2005: Applicability of geophysical prospecting methods for mapping of soil compaction and variability of soil texture on farm land. J. Plant Nutr. Soil Sci. 2005 vol. 168, p. 68-79

Savoie, Muck & Holmes (2004): Laboratory Assessment of Bunker Silo Density Part II:Whole-Plant Corn, Am. Soc. Agr. Eng., year 2004, vol. 20(2), p. 165-171

Shao, Wang, Shimojo & Masuda (2005): Effect of Ensiling Density on Fermentation Quality of Guineagrass, Asian-Aust. J. Anim. Sci., year 2005, vol. 18(9), p. 1273-1278

Williams, A.G., Hoxey, R.P. & Lowe, J.F. (1997): Changes in temperature and silo gas composition during ensiling, storage and feeding-out grass silage. Grass and Forage Science. Vol. 52(2), P. 176, June 1997

The potentials of a novel acoustic sensor approach for determining soil texture and structure

Vicent Gasso-Tortajada[1], Victor Dubasaru[2], Carlos Rojas[2], Torben Brøchner[1] and Ole Green[1]*

1) Department of Biosystems Engineering, Faculty of Agricultural Sciences, Aarhus University, Denmark.

2) Department of Civil Engineering, VIA University College, Denmark.

**) Corresponding author: Ole Green, Ole.Green@agrsci.dk, Research Centre Foulum, Blichers Allé 20, DK-8830 Tjele.*

Introduction

A proper assessment of soil properties is essential for achieving a sustainable agricultural production. The crop yield and the fertilizer application rate are found to be highly dependent on soil texture and structure (Adamchuk et al., 2004). Conventional methods for monitoring soil texture and structure parameters disturb considerably the trial plot and the test samples (Moore et al., 1992). Therefore, the need of using in situ and nondestructive soil monitoring methods increases.

When an air-borne sound wave comes into contact with soil, part of its energy is reflected, another fraction is transmitted through the medium and the rest is dissipated in form of heat due to thermo-viscous effects in the soil pores (i.e. absorption phenomenon) (Voronina et al., 2003). Several studies found that the acoustical behaviour of porous granular media can be described in terms of porosity, air-flow resistivity and tortuosity (Sabatier et al., 1990). As a result, soil texture and structure can be related with the soil acoustic properties. At this time, few studies have used acoustic methods for monitoring physical characteristics of agricultural soils (Sabatier et al., 1990; Moore et al., 1992) and further investigations are needed.

The aim of this study was to establish the base for developing an alternative non-destructive and in situ acoustic technique based on the sound absorption and transmission phenomena for determining soil texture and structure.

Methodology

The sand (0.25-1.60 mm) was dried (24 h, 150 °C) and then sieved according to a standard method (ISO 3310-1) where sieve sizes of 0.25, 0.6 and 1.0 mm were used. The test samples (n=16) were prepared by mixing the sieved fractions in different proportions. Then, the average particle size and bulk density of each sample were calculated.

The absorption coefficient (α) (ratio of absorbed to incident sound energy) and the sound transmission loss coefficient (*TL*) (difference between the incident and the transmitted sound energy, measured in dB) of the sand samples were determined by using two standardized impedance tubes (SCS9020, S.C.S., Italy), each one for a specific frequency range (50-997 and 800-4996 Hz). Two wire mesh sample-holders of 28 and 100 mm of diameter and 200 mm of length were used. α and *TL* spectra were determined by generating white noise at one of the tube extremes and by measuring the sound pressure variations between different microphone positions with respect to the sample. Two different tube configurations for calculating α and *TL* were used. In the α configuration (figure 1a) the pressure variations were measured between the sound source and the sample, while in the *TL* configuration (figure 1b) these variations were measured at both sides of the sample.

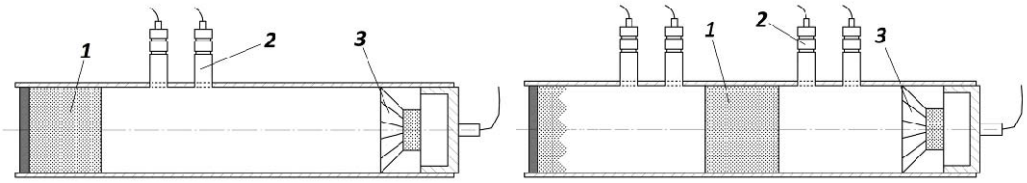

Figure 1. a) Impedance tube in α configuration. b) Impedance tube in TL configuration. Where 1 is the test sample, 2 a microphone and 3 the sound source.

Results and Discussion

According to the analysed spectra, in general, samples with larger average particle size present a higher sound absorption. This finding is in accordance with Voronina et al. (2003) who found the same phenomenon for different granular materials with relatively similar particle size (0.4-3.5 mm). Additionally, investigations in marine sediment sands at ultrasonic frequencies found similar results (Prasad et al., 1992).

It is pertinent to note that the above mentioned phenomenon may be limited to the particle size range analysed in this study. This hypothesis is based on results of acoustic investigations of granular materials with larger particle sizes, such as gravels (2-25 mm) (Swenson et al., 2010) or seeds (1.9-5.5 mm) (Gasso-Tortajada et al., in press), that found an inverse sound absorption behaviour with respect to the particle size.

If the amplitude of the resonance oscillations is analysed, higher amplitudes are found for the larger particle samples. This phenomenon is more noticeable at the high frequencies range. Other studies found similar results for granular materials with larger particle sizes (Gasso-Tortajada et al., in press).

In the case of comparing samples with the same average particle size but different bulk density, the sound absorption appears to be inversely related with density. This fact is associated with the reduction of the pore volume due to compaction.

The correlation coefficients (*R2*) between α and particle size, α and density, and α and the quotient particle-size/density (*s/ρ*) were determined for each analysed frequency. The best correlation was found between α and the quotient *s/ρ* with an *R2* of 0.95 at the frequency of 768 Hz. The correlation between α and particle size was also important, however the sample density did not present any significant correlation.

When *TL* spectra were analysed, an inverse relation between particle size and *TL* was found. In addition, the smaller the average particle size the larger the fluctuations of the *TL* spectra, especially at high frequencies. The best correlation was found between *TL* and *s/ρ* at the frequency of 2009 Hz, corresponding to an *R2* of -0.94.

Conclusions

This investigation has demonstrated that particle size and density are some of the principal governing parameters regarding sound absorption and transmission in soils. Further work will focus on porosity, permeability and water content data. Additionally, more advanced spectral data analysis, i.e. multivariate statistics, will be performed for developing statistical models to classify physical soil properties based on acoustic spectra. In future, acoustic sensors may complement other soil sensors with different target parameters (e.g. near infrared spectroscopy) to develop a more sophisticated nondestructive and in situ soil monitoring method.

References

Adamchuk, V.I., Hummel, J.W., Morgan, M.T., Upadhyaya, S.K., 2004. On-the-go soil sensors for precision agriculture. Comput. Electron. Agric. 44, 71-91.

Gasso-Tortajada, V., Ward, A.J., Mansur, H., Brøchner, T., Sørensen, C.A.G., Green, O. A novel acoustic sensor approach to classify seeds based on sound absorption spectra. Sensors. In press.

Moore, H.M, Attenborough, K., 1992. Acoustic determination of air-filled porosity and relative air permeability of soils. J. Soil Sci. 43, 211-228.

Prasad, M., Meissner, R., 1992. Attenuation mechanisms in sands: Laboratory versus theoretical (Biot) data. Geophysics. 57(5), 710-719.

Sabatier, J. M., Hess, H., Arnott, W.P., Attenborough, K., Romkens, M.J.M., Grissinger, E.H., 1990. In Situ Measurements of Soil Physical Properties by Acoustical Techniques. Soil Sci. Soc. Am. J. 54, 658-672.

Swenson, G.W., White, M.J., Oelze, M.L., 2010. Low-frequency sound wave parameter measurement in gravels. Appl. Acoust. 71, 45-51.

Voronina, N.N., Horoshenkov, K.V., 2003. A new empirical model for the acoustic properties of loose granular media. Appl. Acoust. 64, 415-432.

Measuring spatial distribution of ammonium in plant soil systems using imaging optodes

Niklas Strömberg[1] and Sofia Delin[2].

1) SP, Chemistry and Materials, Sweden, niklas.stromberg@sp.se

2) SLU, Deparment of Soil and Environment, Sweden, sofia.delin@mark.slu.se

Introduction

Studies of the spatial distribution of mineral nitrogen (N) in soil over time at a very small scale have been limited, but would provide information useful for research in plant nutrition. For instance, nitogen release and distribution from different fertilisers, applied with different techniques under different conditions, could be studied. In the same way studies/images of nutrient flow patterns, uptake, adsorption, evaporation and transformation of nutrients close to roots over time would effectively show how plants function in a specific soil. Imaging optodes have the ability to provide images of solutes in two spatial dimensions over time (Strömberg, 2008) and thereby constitute an useful tool for estimates of solute budgets directly in plant-soil systems. In this brief article, we summarise current knowledge on optode sensor technology for ammonium and its use in plant soil systems.

Imaging optodes

Imaging optodes are sensor films which, when in contact with a material or object, visualise the concentration of a substance from time to time. Although the concentration is often seen as increased intensity of the film, special techniques are available to actually translate the light intensity to a concentration of the substance. The optode is usually illuminated with light and photographed with a camera. Today, many commercial digital cameras or cameras for amateur astronomy are sufficient to perform the detection function. Illumination was previously dependent on expensive xenon discharge light sources and bandpass filters, but since the introduction of high powered light-emitting diodes (LEDs), the technical requirements can be met at a fraction of the cost. LEDs also make it possible to design new instruments that can be automated in a way that was practically impossible with light sources based on discharge lamps. The light intensity can be accurately controlled and adjusted electronically and has a narrow spectral band width. Moreover, LEDs are possible to modulate and switch on and off repeatedly, and have at least 50 times longer operational lifetime than discharge lamps.

Ammonium optode

The ammonium optode discussed in this article is based on phase transfer of a fluorescent dye (MC 540) in a emulsion film mediated by changes in ammonium concentrations. More specifically, ammonium ions from the sample diffuse into a hydrogel/ether emulsion film, where they are bound to the cyclic carrier molecule nonactin. Phase transfer of the ammonium-nonactin complex across the hydrogel-ether interface proceeds through simultaneous incorporation of the negatively charged MC 540. MC 540 has optical properties that change excitation/emission fluorescence properties upon shift of solvent. In the sensor configuration applied, excitation/emission maxima were shifted from 520/570 nm in the hydrogel to 570/586 nm in the ether emulsion. Ammonium was quantified through a dual excitation/emission image ratio (excitation:emission / excitation:emission; 572nm:592nm / 520nm:572nm) coupled to a time-correlated pixel-by-pixel calibration procedure. Images displaying ammonium were then treated, for example to calculate threshold levels, gradients and profiles.

a b

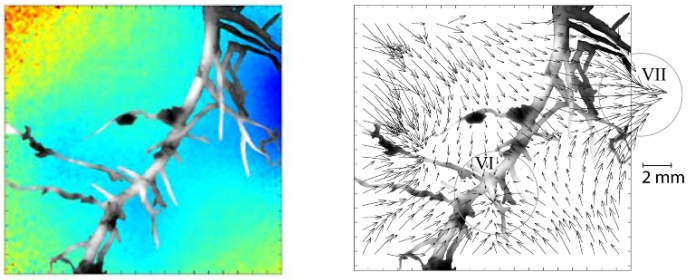

Figure 1. Composite image of the structure of a tomato root and (a) ammonium concentrations visualised by the optode film after one day and (b) ammonium gradients represented by vectors that indicate the flow pattern (Strömberg 2008).

Imaging techniques

In addition to concentration images (Figure 1a), there are several ways to represent the data from optodes. In order to locate active root structures more precisely, quiver plots can be calculated (Figure 1b). A quiver plot displays velocity vectors as arrows with components at each position (pixel) in the image corresponding to the resulting gradient between adjacent pixels. Each arrow represents the average value of 12 by 12 pixels and, consequently, shows where this package of ammonium is heading, as well as the magnitude of the flow (length of arrow). The use of this technique with the ammonium optode made it possible to locate ammonium flow close to small root structures (Figure 1b). The use of threshold values can show pulse effects and uptake processes more efficiently during the day. Figure 2 shows reduced uptake calculated for the same root structure seen in Figure 1. Another way to present data is to show concentration changes in soil profiles over time (Figure 4), which are easier to interpret than the concentration images themselves.

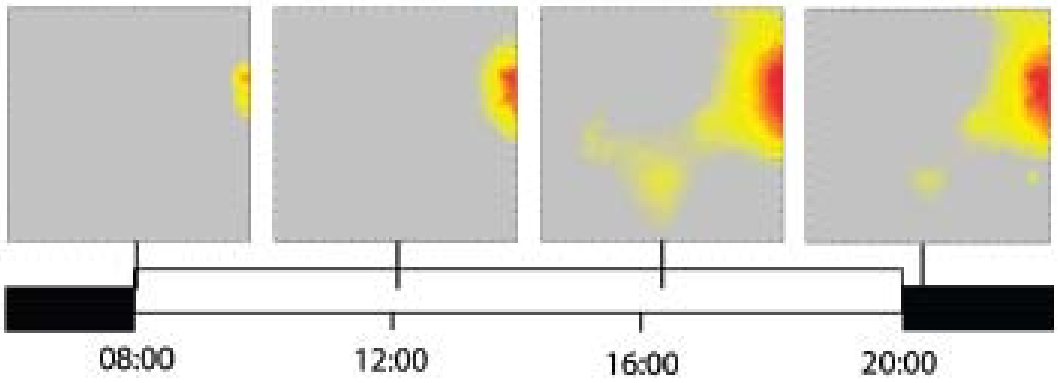

Figure 2. Images showing the development of the depletion zone from morning to evening close to the root structure displayed in Figure 1. The darker colour indicates rapid uptake/ammonium depletion in the reservoir.

Treatments and replicates

A high throughput imaging system based on LED illumination and 24 sample resevoirs (microcosms) has recently been developed (Figure 3; Strömberg et al., 2009). This allows large experiments with replicate samples to be performed automatically over several weeks. In the microcosms, humidity and oxygen content can be controlled. Automatic imaging of solutes over time can be achieved without any labour.

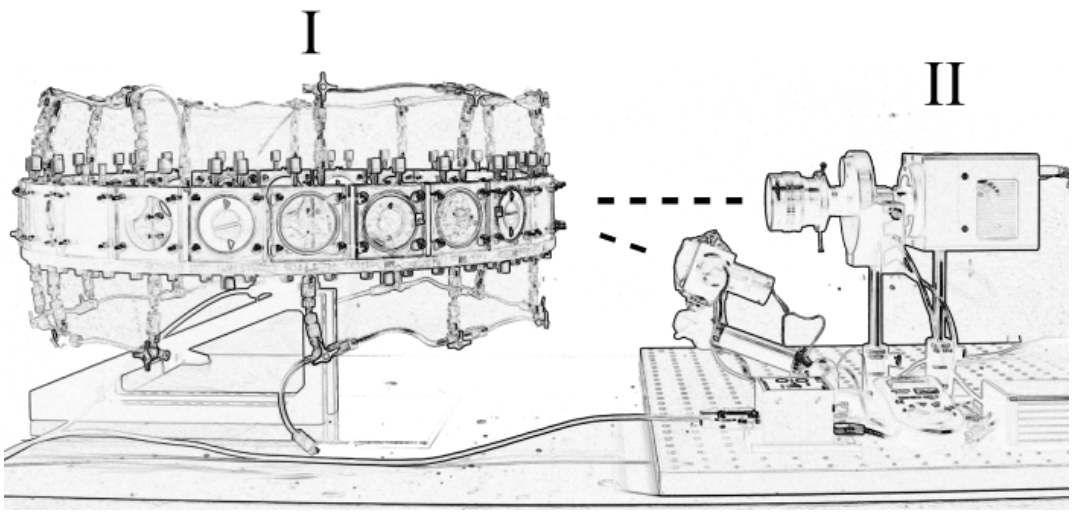

Figure 3. High throughput imaging system for screening of solutes, with 24 microcosms fixed onto a rotating turret (I) in front of the optical system (II).

The turret with 24 separate cells enables comparison of different treatments, with replicates. For instance, spatial ammonium distribution after different degrees of incorporation of solid chicken manure and cattle slurry into soil has been examined by comparing the plotted concentration thorough the soil profile between treatments at different dates (Figure 4; Delin & Strömberg, 2010). The technique proved useful for evaluating ammonium distribution and adsorption, but net N mineralisation required incubations.

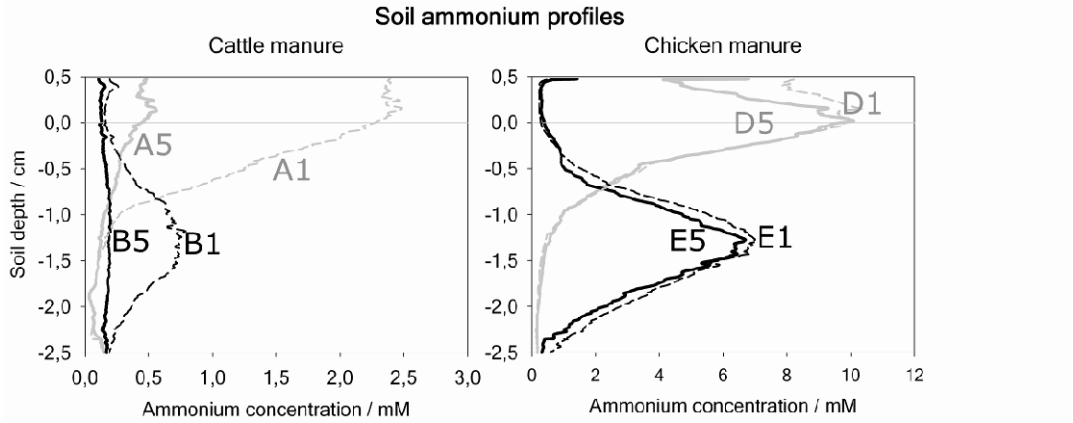

Figure 4. Average ammonium concentration covering a 1 mm wide band cutting through the soil profile at manure application sites of treatments A (cattle slurry on top), B (cattle slurry below soil surface), D (chicken manure on top) and E (chicken manure below soil surface) one and five days after manure application.

In an additional study, ammonium distribution from fertilisers in soils with different soil moisture content was studied. Since the optode requires rather wet conditions, the ammonium distribution could not be studied when the soil was dry. Instead, the cell was kept dry without a sensor for one week before the sensor was fitted. In order to visualise more of the ammonium, an attempt was made to limit adsorption by adding KCl to the soil solution. However, modification with KCl is problematic due to the cross-sensitivity to potassium, which made this attempt unsuccessful.

References

Delin, S. and Strömberg, N. 2010. Imaging-optode measurements of ammonium distribution in soil after different manure amendments. European Journal of Soil Science, in press.

Strömberg, N., Hulth. S 2005. Assessing an imaging ammonium sensor using time correlated pixel-by-pixel calibration. ANAL CHIM ACTA 550:61-68.

Strömberg N. 2008. Determination of ammonium turnover and flow patterns close to roots using imaging optodes. ENV SCI TEC 42:1630-1637

Strömberg, N., Engelbrektsson, J. & Delin, S. 2009. A high throughput optical system for imaging optodes. Sensors and Actuators B, 140, 418-425.

3D-terrestrial laser scanning for the measurement of microtopography on agricultural soils

R.J. Barneveld, MSc.

Wageningen University and Research Centre, Dpt. Environmental Sciences, Chair Group Soil Physics, Ecohydrology and Groundwater Management. c/o Bioforsk Jord og Miljø, Fr. A. Dahlsvei 20, 1432, Ås, Norway.

Phone: +4796851434, E-mail robert.barneveld.@wur.nl

Background and objective

The importance of microtopography for overland flow and its related processes has long been recognised (Römkens and Yang, 1987; Darboux and Huang, 2001). The significance of roughness for hydrological simulation has equally well been documented (e.g. Helming *et al.*, 1998). While laboratory studies (*ibid.*) have indicated that changes in soil roughness during a runoff event significantly influence discharge rates, such studies have not been carried out in field settings. The major constraint for on-site investigations is the absence of a non-destructive methodology to measure microtopography. Methods to characterise microtopography employ either contact (e.g. chain and pins) or non-contact techniques such as photogrammetry and laser scanning (Jester and Klik, 2005). Without exception, they require the observer to approach the object very closely. Even frame-mounted laser scanners need to be installed and operated. An additional constraint is the difficulty of successive measurements of a certain soil surface. In order to take on-site microtopography investigations to a level where they can provide input for the assessment of runoff hydraulics and soil loss and deposition, this difficulty needs to be overcome.

In industrial construction, infrastructure and offshore operations, high definition 3-dimensional terrestrial laser scanning (TLS) devices are used for mapping objects. The research presented here was carried out in order to assess whether or not TLS technology is capable of delivering precise and accurate non-destructive measurements of soil surfaces that can be used to construct terrain models at high spatial resolutions (0.01 to 0.20 cm).

Materials and methods

For this purpose, two experiments were undertaken; one in a laboratory setting with a standard sized object, and one on-site at a tilled field. The laboratory set-up consisted of a set of toy construction bricks with perpendicular angles and rough horizontal surfaces. They were built up on top of a table to a fully anisotropic shape, i.e. with no height gradient in the x-direction and a regular variation in height along the y-direction. The rectangular base of the object was 0.190 m wide and 0.095 m long. The shape was scanned with a Leica ScanStation that uses a pulsed laser signal to determine the distance to a point and simultaneously with the angles in the horizontal and vertical planes. In order to minimise the data gaps that result from the shadow the shape itself casts in the direction of observation, measurements were repeated from two different positions. All points of view were located 4 to 5 m from the object. The resulting point clouds were exported separately to a ASCII file with x, y and z (height above a reference surface) values for further treatment. The three point clouds were also merged with Leica's scanner operation and data processing software and exported as such.

The field trial was undertaken on a newly sown wheat field in Akershus fylke, south-eastern Norway. A 2.53 by 3.36 m plot was scanned from three viewpoints and data were exported in a similar fashion as in the laboratory trial.

Data processing consisted of two steps: loading the point clouds into a georectified grid of variable resolutions and filtering. Filtering was required in order to eliminate outliers that disturbed the average height value after importing. A simple, surface based filter was developed, tested and applied. Data quality parameters were formulated and data analysis was carried out on the point cloud from the laboratory trial and a selected set from the field trial. Parameter formulation was based on two possible uses for which TLS scanning could be applied; terrain model (DTM) building and the abstraction of geomorphological descriptors, such as roughness and isotropy.

For the laboratory trial, a Welch t-test was carried out for each grid cell, testing the mean value of the scan against the actual, digitally reconstructed, shape. The morphological descriptor used to assess the similarity of the measured and actual objects was two-dimensional tortuosity, i.e. the ratio between the actual surface area of the object and the surface area of its base.

For the field trial, the zero-hypothesis could not be tested against a given model of the actual surface. Instead, the three point clouds were tested against each other. The assumption here was that any measuring error or bias would emerge from such a comparison. Once again, for purposes of testing the suitability for DTM construction, a t-test was carried out in each grid cell. A local slope-based morphological descriptor was used. Slope values were calculated in two directions in each grid cell and aggregated for the entire scanned surface area. Since the soil surface of tilled agricultural soils is rough, coverage (defined as point count per grid cell) was also assessed.

Since the resolution of the grid in which data were imported was assumed to affect data quality, grid cell dimensions for the laboratory experiments ranged from 2 to 15 mm, and for the field trial from 2 to 15 cm.

Results

Visual inspection showed that the laboratory scan required data manipulation to eliminate outliers. The source of the outliers has yet to be determined, but could be due to the fact that the laser beam width is non-zero (Lichti and Skaloud, 2010). After filtering however, the statistical parameters of the scanned surface resembled those of the modelled object fairly well. It was found that performance was best for grids with a resolution between 2 and 3 mm (standard deviation of the errors 5.1×10^{-3} m). The ratio of cells that had a significantly different estimate of the height z ($p<0.01$) was 0.211 (rapidly increasing with lower resolutions). The ratio between the tortuosity of the scanned and that of the modelled object was 1.05 (improving slightly for lower resolutions).

For the field trial the resolution for data processing and analysis was set at 2 cm. Filtering was required and carried out to remove artefacts. The coverage of the scan was excellent at the given resolution; a ratio of merely 4.8×10^{-5} of the cells were not covered by any of the three viewpoints. The average count of observations per grid cell for the combined cloud was found to be 32.2. The ratio of cells that showed significantly different estimates of the height z ($p<0.01$) in comparison to the other point clouds ranged from 0.194 to 0.257. The standard deviation of the residuals equalled 2.2×10^{-2}. As for morphological data quality, aggregated slope values were structurally lower for the combined point cloud in comparison to the individual clouds. This would indicate a smoothing effect on the final DTM that may not be justified.

The scanning process took little time; 20 minutes for a scan from a single viewpoint was the maximum. After the development of the appropriate algorithms, data processing, filtering and analysis was very fast.

Conclusion

The application of the TLS technology in combination with the appropriate data processing methods has yielded useful results. Not only were data of sufficient quality to render them highly suitable for surface characterisations and high resolution DTM construction, they also enable researchers to repeat measurements in the field, and obtain quantitative indications of soil surface dynamics. There are however three considerations to be taken when applying terrestrial laser scanning for field studies. The first is that data quality is likely to be highly dependent of relative aspect, i.e. the vertical angle between the scanning device and the soil surface. Relative aspect is a function of tillage, soil structure, time, field inclination and the height above the surface of the point of view. Secondly, a simple filter has performed well on a sparsely vegetated soil surface. A denser plant cover will reduce the efficacy of such filters, and from a certain density, vegetation will obscure the soil surface to a degree at which DTM construction is not feasible any more. Thirdly the relatively high standard deviation obtained in the field trial prescribes careful interpretation of results, especially when sequences in time of a certain plot are concerned.

Recommendations for further research include: testing the methodology on soil surfaces with different morphological characteristics, improving filtering techniques for vegetation removal and applying the methodology for sequential recordings of the soil surface over the year and/or years.

References

Darboux, F., Huang, C., 2001. Contrasting Effects of Surface Roughness on Erosion and Runoff . In: Ascough II, J.C, Flanagan , F.C. (Eds.), Soil Erosion Research for the 21st Century. Proceedings of the International Symposion of ASEA, 3-5 January 2001, Honolulu, HI, USA.

Jester, W., Klik, A., 2005. Soil surface roughness measurement - methods, applicability, and surface representation. Catena 64, 164-192.

Helming, K., Römkens, M.J.M., Prasad, S.N., 1998. Surface Roughness Related Processes of Runoff and Soil Loss: A Flume Study. Soil Sci. Am. J. 62, 243-250.

Römkens, M.J.M., Yang, J.Y., 1987. Soil roughness changes from rainfall. Trans. ASAE 30, p. 101-107.

Lichti, D., and Skaloud, J., 2010. Registration and calibration. In: Vosselman, G., Maas, H.G. (Eds.), 2010. Airborne and Terrestrial Laser Scanning. CRC Press LLC, Boca Raton, USA.

Methods for measuring crop damage in grassland after use of knife/tine slurry injection equipment

Halling M.A.[1], Rodhe L.[2] and Rydberg A.[2]

1) Department of Crop Production Ecology, Swedish University of Agricultural Sciences, Box 7043, SE 750 07 Uppsala, Sweden, +46 18 671429, magnus.halling@vpe.slu.se

2) JTI – Swedish Institute of Agricultural and Environmental Engineering, Box 7033, SE 750 07 Uppsala, Sweden, +46 10 5166951, lena.rodhe@jti.se, anna.rydberg@jti.se

Introduction

Slurry injection into grassland has advantages over slurry spreading as it decreases ammonia losses and odour and improves forage hygiene. However, injection may harm grassland plants (Rodhe *et al*., 2006), although knife-based equipment is used on lawns to stimulate growth. In order to be able to identify crop damages as well as to predict negative influence on yield by using different types of knives/tines, there is a need of measuring methods. The objective of this study was to evaluate traditional as well as new methods for measuring crop damages caused by knives/tines in grassland.

Material and Methods

Different methods were used to measure crop damage during growth in order to predict yield decreases due to knife/tine damage. In split-split-plot field experiments, four different types of knife/tine equipment were tested on three different grassland swards, with or without added nitrogen. In two separate experiments, the injection treatments were applied in spring (late April) or after the first cut in mid-June.

The methods where traditional ones as 1) Sward cover of seeded species, 2) tiller weight, but also 3) canopy temperature measured with a thermal camera (FLIR P62) and 4) leaf area index (LAI) measured with LAI-2000 Plant Canopy Analyzer (LI-COR® Biosciences). All methods were used two weeks after treatment.

Principal component analysis (PCA) was made by using the program CANOCO version 4.5 (ter Braak and Šmilauer, 2002). In the PCA, the relationships between sward assessment variables and yield characteristics were analysed. Mean values were used and each trial was analysed separately.

Results

The results from the PCA showed that there in most cases were a high correlation between the yield following treatment and LAI measured two weeks after treatment but also the Sward coverage and Amount of tillers could indicate the rate of crop damage and thereby forecasting the yield decrease. The sward coverage two weeks after injection and just after the following cut had also a rather good correlation. Measuring of sward surface temperature had a negative correlation with yield, which means that the higher temperature, the lower yield.

Conclusions

LAI, crop temperature and sward assessment can predict yield reduction relative to no treatment (or detect crop damages).

References

Rodhe L., Pell M. & Yamulki S. 2006. Nitrous oxide, methane and ammonia emissions following slurry spreading on grassland. Soil Use and Management 22, 229-237.

ter Braak CJF, Šmilauer P (2002) CANOCO reference manual and CanoDraw for Windows user's guide: software for canonical community ordination (version 4.5). Microcomputer Power, Ithaca.

Detection of urine patches on grassland with an electromagnetic induction-based sensor

Lena Rodhe, Eva Salomon and Mikael Gilbertsson*

JTI – Swedish Institute of Agricultural and Environmental Engineering, Box 7033, SE-75007 Uppsala, Sweden.

**) Correpsonding author, E-mail: lena.rodhe@jti.se.*

Abstract

The aim of this study was to study if it is possible to map the urine patches after grazing animals by measuring the electrical conductivity (EC) of the upper soil by using an EC meter. The objectives were to estimate: 1). The detection levels for increasing applied amounts of urine. 2. The ability to detect applied amounts of urine over time on the grassland. 3. If there was any correlation between soil conductivity and amounts of mineral-N in the topsoil. The artificial urine was spread on grassland at different application rates corresponding to 620, 1250, 2500, 5000 and 10000 kg N ha^{-1} on the 28th of June. The experiment was organised in a randomised block design with three replicates. Sampling of soil and measurements of the soil EC in each plot were conducted eight and 44 days after spreading. The EC was measured with a commercial meter (EM-38; Geonics Ltd.). Electromagnetic induction measurements could be used to detect areas with high nitrate content on grassland both eight and 44 days after fertilising. However, the threshold for detecting differences is high, about 600 kg N ha^{-1}. The correlations between soil EC and amounts of mineral-N in the topsoil were rather high.

Introduction

On arable fields, which recently have been used for grazing, it is desired to determine the spatial distribution of mineral N as it could vary very much depending on the excretion behaviour of the animals. The N-fertilising could then be adjusted and spatially dosed according to the mineral N content of the upper soil and the need of the crop. This will promote less leakage and good economy. According to Stevens *et al*. (1995) the dominant ions in slurry are ammonium nitrogen (NH_4^+) and potassium (K^+). In the soil the NH_4^+ mineralize mainly to nitrate (NO_3^-). The electrical conductivity (EC) is a reliable indicator of NO_3-N in the soil (Eigenberg & Nienaber, 2003) and has been used for detecting hot spots of mineral N. The N loading rate at an individual urine patch is equivalent to about 1000 kg N ha^{-1} (Haynes & Williams, 1993).

The hypothesis is: It is possible to map the urine patches after grazing animals by measuring the electric conductivity of the upper soil by using an electrical conductivity meter. The objectives were to estimate: 1). The detection levels for increasing applied amounts of urine on grassland. 2. The ability to detect applied amounts of urine over time on the grassland. 3. If there was any correlation between soil conductivity and amounts of mineral-N in the topsoil.

Material and Methods

Artificial cattle urine (ACU) was made by mineral nitrogen (N) and potassium (K) added to water in the proportion corresponding to the N- and K-contents of fresh cattle urine (1.24% N and 1.2% of K). Mineral fertilisers used were Calcinit (16% N) and Krista K Plus (13.7%N and 16% K) from Yara®. The artificial urine was spread on grassland at different application rates corresponding to 620, 1250, 2500, 5000 and 10000 kg N ha^{-1} on the 28th of June, Table 1.

Table 1. Treatments and applied amounts in kg N ha^{-1} and tonnes ha^{-1}

Treatments	Application	Kg N ha^{-1}	Tonnes ha^{-1}
A	No application	0	
B	Water irrigated, same amounts as treatment F	0	403
C	Artificial cattle urine (1.24% N, 1.19% K)	620	50
D	Artificial cattle urine (1.24% N, 1.19% K)	1250	101
E	Artificial cattle urine (1.24% N, 1.19% K)	2500	202
F	Artificial cattle urine (1.24% N, 1.19% K)	5000	403
G	Artificial cattle urine (1.24% N, 1.19% K)	10000	806

Differences between treatments per experiment were analysed using a General Linear Model (GLM) in the statistic package SAS 6.12.

A treatment with no fertiliser was also included as control as well as an irrigation treatment of 40 mm (400 tonnes ha^{-1}), the same amount as the treatment 5000 kg N ha^{-1}. The grassland had not been fertilised earlier in the year. The soil was classified as a clay soil with 42% clay content and 1.7% organic matter. The experiment was organised in a randomised block design with three replicates with a small plot size of 3 by 3 m. There was an inter-space of 3 m between each small plot within the blocks. Sampling of soil and measurements of the soil EC in each plot were conducted eight and 44 days after spreading. Ten soil cores from each plot, representing 0-30 cm depth, were sampled and thoroughly mixed, deep-frozen (-20°C) until analyses of NH_4-N and NO_3-N content. The electrical conductivity was measured with a commercial soil electrical conductivity meter (EM-38; Geonics Ltd.), and the sensor was placed in a horizontal position, Figure 1. Thereby two third of the response originated from a soil depth less than 0.75 m. The measurement with the EC sensor was done by placing the sensor in the middle of each plot and measuring the EC for at least one minute. The sensor was calibrated once an hour in a plot specially intended for this.

Figure 1. Measuring the electrical conductivity with a commercial soil electrical conductivity meter (EM-38; Geonics Ltd.) eight days after spreading. The grass turned into yellow in the plots with the highest nitrogen rates.

Results and discussion

The measured EC increased with increased application rate at the first (Figure 2) and second measurements after spreading.

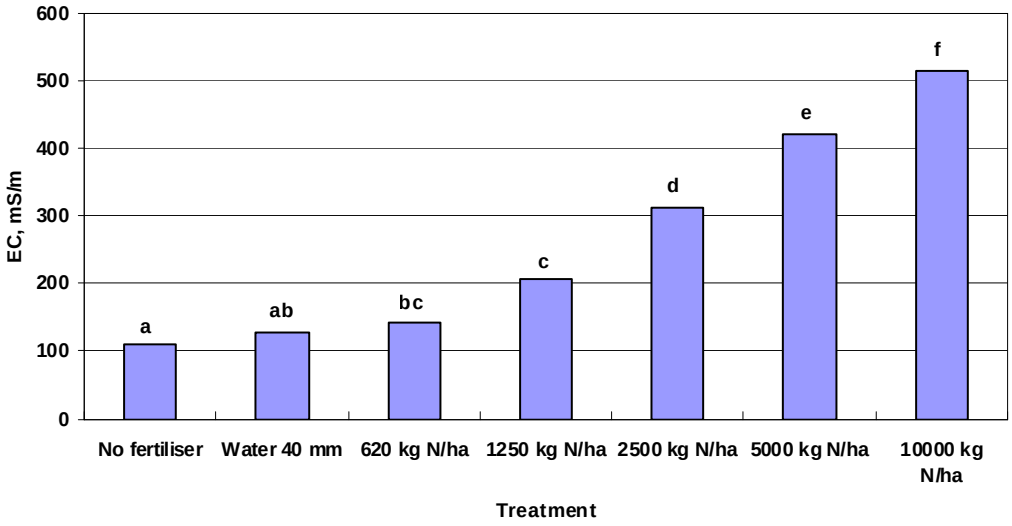

Figure 2. Soil electrical conductivity (mS m^{-1}) eight days after spreading for the different treatments measured with Geonics EM-38. Bars with different letters are significantly different (P<0.05).

However, it was not possible to show significant differences between treatments with 620 kg N ha^{-1} and 1250 kg N ha^{-1} nor between irrigated without fertiliser and fertiliser 620 kg N ha^{-1}. It means that the accuracy is not in the range of conventional fertilizer rates. Eigenberg & Nienaber (2003) used the method to an abandoned manure handling site to determine nutrient build-up and it has also been used to locate seepage from animal waste lagoons.

The differences in soil EC between the treatments were about the same at the later measuring, 44 days after spreading, as eight days after spreading. In between the measurements there had been 202 mm rain, which seemed not to have decreased the differences. There was a correlation between measured EC and mineral N content of the soil with a R2 value of 0.79 eight days after spreading and a R2 of 0.77 44 days after spreading.

Conclusions

Electromagnetic induction mesurements could be used to detect areas with high NO_3 content on grassland both eight and 44 days after fertilising. However, the threshold for detecting differences is high, about 600 kg N ha^{-1}. The correlations between soil electrical conductivity and amounts of mineral-N in the topsoil were rather high at the two times of measuring with R2 values of 0.79 and 0.76, respectively.

References

Eigenberg R.A., Nienaber J.A. Electromagnetic induction methods applied to an abandoned manure handling site to determine nutrient buildup. Journal of Environmental Quality 2003, 32, pp. 1837-1843.

Haynes R.J., Williams P.H. Nutrient cycling and soil fertility in the grased pasture ecosystem. Advances in Agronomy 1993, 49, pp. 119-199.

Stevens R.J., O´Bric C.J., Carton O. Estimation nutrient content of animal slurries using electrical conductivity. Journal of Agricultural Science, Cambridge 1995, 125, 233-238.

Platform for integrating ICT and automation

Claus G. Sørensen[1], Frank W. Oudshoorn[1], Ole Green[1], Dionysis Bochtis[1], Lars Munkholm[2], Anton G. Thomsen[2] and Ibrahim Hameed[1]

1) Department of Biosystems Engineering, University of Aarhus

2) Department of Agroecology and Environment, University of Aarhus

Research Centre Foulum, Blichers Allé 20, DK-8830 Tjele

Corresponding author, E-mail:claus.soerensen@agrsci.dk

The Faculty of Agricultural Sciences of Aarhus University, Denmark, has initiated the design and establishment of a 24 ha research platform on future organic arable cropping (OAC) systems based on an extended use of information and communication technologies (ICT) and adaptable cognitive automation. The overall mission of the platform will be to enhance OAC systems in terms of documentation quality, process activities, and labour environment and increase the overall system's efficiency while at the same time maintain its environmental benefits such as biodiversity and reduced fossil energy consumption. Fused information from the geographical information system (GIS) is accessible online through on-board interfaces, with the real-time information provided by on-the-go sensors (e.g. on-board micro climate station). Furthermore, the platform will be the basis for the documentation of traffic impact as positioning coordinates are coupled with tire pressure, axel load and monitored data for every job carried out in the field.

Different research studies and applications can be enhanced by using GNSS and various sensor technologies combined with a stable research platform with a well documented history and monitoring system. Especially for long term effects, site specific impact, and a pursued system approach, the platform is of value. OAC systems are dependent on optimal soil structure and economically and environmentally justified site specific application techniques. Therefore, it is a logical step to develop innovative and ICT based management focusing on time, labor, machinery and system optimization. The platform is divided in three equally sized fields of 8 ha, representing a typical arable crop rotation for Danish organic growers (clover grass-high value cereal/rapeseed (canola)/ row culture-low value cereal). The crop sequence reflects the degressive nutritional status of the soil, as organic fertilizer is rationed. OAC systems are dependent on available nutrients from organic husbandry, which can only be imported in limited amounts. Often organic husbandry is in need of nutrients themselves

In this paper, design of the system, support measures, and the design of the information flow will be elaborated. The prospects for research, system optimizations, task time modeling of labor and machinery and automated spatially adaptable equipment will be addressed.

Significant Effects of the Machine Wheel Load on Grass Yield by Using a New Field Experimental Method

Ole Green[1], Rasmus N. Jørgensen[2], Kristian Kristensen[3], Dionysis Bochtis[1] and Claus G. Sørensen[1]*

1) Department of Biosystems Engineering, Faculty of Agricultural Sciences, University of Aarhus, Denmark

2) Institute of Chemical Engineering, Biotechnology and Environmental Technology, Faculty of Engineering, University of Southern Denmark, Denmark

3) Department of Genetics and Biotechnology, Faculty of Agricultural Sciences, University of Aarhus, Denmark

**) Corresponding author, E-mail: Ole.Green@agrsci.dk,* , Address: Research Centre Foulum, Blichers Allé 20, DK-8830 Tjele

Introduction

The increasing weight and size of modern machinery makes the risk of soil and crop damages even more eminent. Therefore, this study was conducted to supplement the existing results of using lighter machinery (Frost 1988a; Frost 1988b) to include the ramifications of using heavier machinery and ensuring an updated decision support to farmers. However, even more importantly the project founded the basis for a new way of performing field experiments, when parameters that normally have difficulties in getting significant results are examined. This paper focuses on the statistical approach of the possibilities with this new field experiment design.

Methodology

The field was located at the Organic Research Centre Rugballegaard, Denmark ([55.864067° N, 9.800732° E]). The area of the field was approximately 14.5 ha and was grown with a grass-clover mixture consisting of 32% tetraploid perennial ryegrass, 50% diploid perennial ryegrass, 10% red clover, and 8% white clover. The grass-clover crop was established in early April 2007 using Autofarm Autosteer RTK-GPS auto steered tractors and the plots had not been trafficked since august 2006. Furthermore, the plots were turned 35 degrees to minimize the risk of bias errors from old traffic lanes.

Experimental design – Each net plot measured 9 x 1.5 m and the treatments were completely randomized onto the field. The plots were placed in pairs where the distance between the two plot centres was 3 m. The 4 treatments were performed in 2008.

Traffic simulations – A Claas Axion tractor equipped with RTK-GPS auto steering and a 15 m3 Kimadan slurry tanker mounted on two axels were used to perform the simulated traffic treatments in the plots. The used machine combination had all 4 axels of the tractor and the slurry trailer traversed, each plot affecting the centreline of the plot in the longitudinal direction. The specific load of each wheel for the low load simulation amounted to 2805 kg for the tractor front wheel load, 2865 kg for the tractor rear wheel load, 1775 kg for the trailer front wheel load, and 1760 kg for the trailer rear wheel load. Opposed to this, the specific load of each wheel for the high load simulation mounted to 2335 kg for the tractor front wheel load, 4745 kg for the tractor rear wheel load, 4435 kg for the trailer front wheel load, and 4435 kg for the trailer rear wheel load. Each traffic was defined as a combination of tyre inflation pressure (100 kPa or 250 kPa) and wheel load (3 Mg or 5 Mg), and a treatment without traffic was carried out. At the time of harvesting, the reference treatment (without traffic) was replicated 242 times.

Yield measurements – The harvesting operation was performed using a Haldrup plot harvester modified with a RTK-GPS system similar to the systems used on the tractors. The working width of the harvester was 1.5 m and the plots were harvested at 2 times (May 14th and 15th 2008). The harvest yield was converted from kg plot-1 to Mg ha-1, and there were not any adjustments for water content.

Statistical analysis – The yield in fresh grass (Mg ha-1) was analysed in a model that included the effect of the treatment, the block effect describing the difference between the previous two fields, the harvest date, the effect of location, the effect of altitude, the effect of the measured EM38, and the distance to forest and hedges close to the north, south and east borders of the field. Mathematically, the model may be written as:

$$Y_i = \mu + \alpha_{t(i)} + \beta_{b(i)} + \gamma_{d(i)} + \delta_1 x_i + \delta_2 x_i^2 + \delta_3 y_i + \delta_4 y_i^2 + \delta_5 x_i y_i + \tau_1 z_i + \tau_2 z_i^2 + \lambda_1 n_i + \lambda_2 s_i + \lambda_3 e + \eta_1 m_i + \eta_2 m_{i\,i}^2 + E_i$$

where

Y_i is the recorded and normalised yield from plot *i*

x_i and y_i ist the center coordinate of plot *i*

z_i is the nean altitute of plot *i*

n_i, s_i and e_i is the logarithm of the distance to wood, trees and hedge in the north, south and east direction

$\mu, \alpha_{t(i)}, \beta_{b(i)},$ and $\gamma_{d(i)}$ is the intercept, the effect of the factors: treatment, block and harvest day

$\delta_1 - \delta_5$ is the linear and quadratic effects of the coordinates and the interaction between the coordinates

τ_1 and τ_2 is the linear and quadratic effect of the mean altitude

λ_1, λ_2 and λ_3 is the linear effect of logaritmic distance to tree in the north, south and east direction

η_1 and η_2 is the linear and quadratic effect of the mean EM38 recordings

E_i is the random effect of plot *i*, which is assumed to be independent and normal distributed with mean zero and constant variance, σ^2.

The variation caused by variations in soil properties was estimated as the joint effect of blocks, coordinates, altitude, distance to trees and EM38 measurements assuming that all plots were traffic free:

$$P_i = \mu + \alpha_1 + \beta_{b(i)} + \delta_1 x_i + \delta_2 x_i^2 + \delta_3 y_i + \delta_4 y_i^2 + \delta_5 x_i y_i + \tau_1 z_i + \tau_2 z_i^2 + \lambda_1 n_i + \lambda_2 s_i + \lambda_3 e_i + \eta_1 m_i + \eta_2 m_i^2$$

Similarly, the yield caused by the location of each plot was predicted by using information about the location of each plot (i.e. by leaving out the last two terms).

All analyses were performed by using the mixed procedure of SAS and the parameters were estimated and tested by using the method of restricted maximum likelihood (REML).

Results

The first statistical analyses revealed two plots with very deviating results. These results were excluded from further analyses.

An attempt was made to improve the model by allowing the random effect, i.e. to be spatially correlated by using different models. However, this did not improve the model.

Yield losses The analyses showed significant effects of the treatment, and that the yield in the field depended on the location of the plot (x and y coordinates and altitude), the distances to trees as well as the treatment history of the two fields (block effect), the EM38 recording and the day of harvest (Table 2).

Table 2 Analysis of variance table and additional contrasts after the model has been reduced

Effect	**Numerator degree of freedom**	**Denominator degree of freedom**	**F-value**	**Pr > F**
Block	1	707	16.21	<.0001
X	1	707	6.04	0.014
x^2	1	707	3.39	0.07
Y	1	707	17.72	<.0001
y^2	1	707	64.93	<.0001
EM38	1	707	33.68	<.0001
$EM38^2$	1	707	18.85	<.0001
Altitude	1	707	13.46	0.0003
$Altitude^2$	1	707	29.57	<.0001
Log distance to forest, North	1	707	35.76	<.0001
Log distance to tree, South	1	707	35.73	<.0001
Log distance to hedge, East	1	707	7.69	0.006
Contrasts				
Wheel load	1	707	9.06	0.003
Tyre inflation pressure	1	707	0.09	0.76
Wheal load×tyre inflation	1	707	1.30	0.26

a) Test of net loss of damaging different individual areas instead of damaging the same area two or four times

b) Test of additive effect for repeated treatment of the same area

The adjusted average yields of all treatments are shown in Table 3 together with an indication of the treatments that are significantly different. The average yield of plots that were not subjected to traffic was 23.3 Mg ha-1. None of the treatments involving traffic had an average yield that was significantly larger than that. All treatments involving traffic and carried out in the year of harvest or carried out more than once had yields that were significantly lower than the treatments not involving any traffic.

Table 3 Effect and standard deviation for each treatment

Treatment no	Time	Wheel Load, kg	Tyre Inflation Pressure, kPa	Estimate, Mg ha^{-1}	Standard error, Mg ha^{-1}	Significant differences[a]
1	-	-	-	23.3	0.19	a b
11	D	4745	100	18.2	0.53	f g
12	D	4745	250	18.7	0.49	e f g
13	D	2865	100	20.0	0.52	d e
14	D	2865	250	19.5	0.52	e f

a) Treatments with same letter(s) are not significantly different at the 5% level using t-tests

The analysis showed that there were not any significant interactions between the factors wheel load and tyre inflation pressure (all P-values larger than 0.2567) – and also there was not any significant effect of tyre inflation pressure (P=0.7624). Thus, the effects can be summarised as the main effect of treatment time and wheel load (Table 2). The wheel load had a significant effect. At all times, the yield was lower when using a wheel load of 5 Mg compared to a wheel load of 3 Mg.

The negative effect of compacting the same area by applying two slurry applications was significantly greater than compacting the same area by the application of two harvests (Table 2). Additional use of the same track (at two harvesting and two slurry applications) further decreased the yield (Table 2).

The soil texture showed a large variability in the experimental field indirectly indicated by the EM38 or the soil conductivity measured within each parcel. The predicted yield for traffic free treatment in all plots varied between 16 and 35 Mg ha-1. A large part of this variation could be identified as being dependent on the location of the plot–coordinates, altitude and distance to trees. Also, the EM38 recordings explained a large part of the variation in the data as the contribution for these recordings varied between approximately -2.5 and 2.0 Mg ha-1.

The yield depended significantly on the day of harvest and was estimated to be 1.4 Mg ha-1 larger in average (SE=0.32 Mg ha-1) on the second day of harvest compared to the first day of harvest.

The inclusion of the covariates reduced the residual standard deviation from 3.8 Mg ha-1 to 2.8 Mg ha-1. Average standard errors on pair wise treatment comparisons were reduced by approximately 25% by including the covariates in the analysis.

Discussion

The compaction and crop damage performed in the experiment had a variable axel load, with the maximum load close to the load used by Frost (1988). Similarly, the maximum tyre inflation pressure is also close to the maximum pressure used in the experiment, therefore allowing the comparison with the results from Frost (1988). The high load treatment gave a yield reduction of 21.89% at 100 kPa and 19.74% at 250 kPa compared to the zero traffic treatment which is close to the 23% by Frost (1988). The yield variation in the field was very large. In order to increase the precision of the estimated treatment effect, several covariates were included. The adjustment of those covariates introduced some uncertainty and created a bias in the adjustment. However, the difference between the treatment estimates before and after the adjustment for soil heterogeneity was generally small.

Conclusion

The following interesting conclusions can be drawn from the experiment:

When comparing the effect of wheel load and tyre pressure, a high wheel load of 5 Mg always results in a significantly higher yield loss compared to the low wheel load of 3 Mg, whereas a high tyre pressure does not give a significant loss compared to a low tyre pressure.

Traffic in early spring, as simulated by slurry distribution, results in yield losses of up to 22%, with the highest losses at the highest wheel load. The low wheel load gave a yield loss of up to 16%.

References

Frost, J.P. (1988a). Effects on crop yield of machinery traffic and soil loosening. 1. Effects on grass yield of traffic frequency and date of loosening. Journal of Agricultural Engineering Research, 39(4) p. 301–31

Frost, J.P. (1988b): Effects on crop yield of machinery traffic and soil loosening. 2. Effects on grass yield of soil compaction, low ground pressure tyres and date of loosening. Journal of Agricultural Engineering Research, 40 (1): 57–69.

Automatic GNSS referred Image Acquisition in Field Experiments

Ole Green[1] and Rasmus Jørgensen[2]

1 Department of Biosystems Engineering, Faculty of Agricultural Sciences, University of Aarhus, Denmark

2 Institute of Chemical Engineering, Biotechnology and Environmental Technology, Faculty of Engineering, University of Southern Denmark, Denmark

Corresponding author: Ole Green, Ole.Green@agrsci.dk, Research Centre Foulum, Blichers Allé 20, DK-8830 Tjele

The objective of this work is to automate field experimental data logging. This will be exemplified by taking color images with a camera pointing directly downwards such that the image fields on the soil surface follows each other closely such that the field is covered with images. Each image is labeled with its position in UTM co-ordinates obtained from the GPS system.

A 14 hectare full scale grass-clover field trial with 24 different traffic intensities and 35 replicates was established. Each net parcel measured 9 x 1.3 m and the 24 treatments were randomized onto the 840 net parcels. The grass clover was established in the spring 2007 using RTK-GPS auto steered tractors and implements. A Claas Axion tractor equipped with an AutoFarm RTK AutoSteer guidance system was used to carry two parallel mounted cameras over the net parcels at a speed of 1 m s^{-1}. In combination, the cameras sampled an area of 1.3 x 0.48 m with 2.1 Hz ensuring that the whole parcel was imaged. Each image was geo-positioned. The image analysis comprised two steps: Extraction of green material and discrimination of grass and clover using the morphological opening approach.

In order to perform this job a tractor was equipped with a boom extending 3 m sideways. Two cameras (AVT Marlin F-046C) were mounted on the boom at a height of 0.9 m and pointing vertically downwards. One camera was mounted at the end of the boom and the other one with the image width closer to the tractor. For each camera, the image field on the soil surface was 0.75 x 0.56 m. In this way, the images covered a swath of 2 x 0.75 m well to the side of the tractor's tracks.

The cameras were controlled by a computer which triggered the cameras at the correct times as the tractor moved over the field. Thereafter, the images were fetched into the computer, labeled with the actual co-ordinates and stored on a large hard disk.

The program system consisted mainly of 2 parts running in parallel. The one part continuously obtained data from the tractor's GPS system and extracted the current position and the forward velocity. These data were stored in a shared memory continuously replacing the previous values.

The other part of the program system triggered the cameras simultaneously each time the tractor moved a distance equal to the image height of 0.56 m. The trig time was calculated from the moment the current forward velocity was obtained from the shared memory. The images were transferred to the computer memory through a high speed Firewire channel. When the image transfer was ready it was labeled with the current position that was also obtained from the shared memory and moved to the hard disk for later analysis. After this procedure, the computer was ready for triggering the next images.

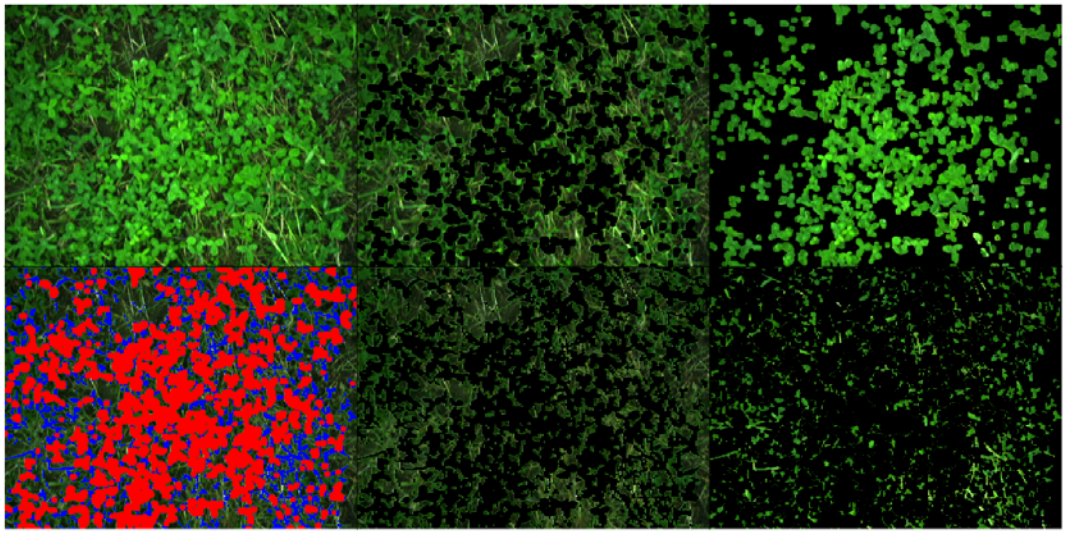

Clover: 38% - Grass: 14% - NotCloverNorGrass: 48%

Measuring and modeling of draught force variations during tillage operations

*Andrés Villa-Henriksen, Gareth Edwards, Frank W. Oudshoorn and Ole Green**

Department of Biosystems Engineering, University of Aarhus, Research Centre Foulum, Blichers Allé 20, DK-8830 Tjele

**) Corresponding author, E-mail: Ole.Green@agrsci.dk*

Introduction

The study of draught forces in tillage operations can bring important information about energy consumption in one of the greatest energy consuming operations in agriculture. A proper knowledge of these forces can reduce fuel costs and decrease CO_2 emissions.

The relation between draught forces and different soil types can also predict the energy consumption in each field according to its soil type. Knowing this relation between draught forces and soil type, the application of sensors in the implement makes it possible to map the field according to its draught force variations and consequently, its soil texture variation.

Background

The factors relating to soil conditions include soil classification (loamy, sandy, etc.), moisture content, previous crop, fertilizer operation, soil resistance and soil compaction. Nyord et al 2010 found that draught forces were heavily affected by the classification of the soil, such as loamy sand, sandy loam and sandy. The draught forces experienced in sandy loam soil were found to be almost double than those in sand. Soil moisture content has been suggested as a factor on the draught force by V. S´anchez-Gir´on 2005 in that it helps the soil becoming more rigid and resistive to be broken up during tillage.

A.P. Onwualu, K.C. Watts 1998 shows that draught force is a factor of vehicle speed and speed squared. However, other reports have suggested that draught force is only a factor of the speed. In this analysis both the speed and the speed squared will be considered as factors and they will be tested to see which is significant.

Materials and methods

The field where the experiment is going to take place is located in Foulum (Denmark) and is a 25 ha organic arable cropping area that has been divided in three equal surfaces containing three different crops.

Sensors and data logger

The sensors will be located in the linkage in a structure like the three point hitch and placed in between the tractor and the implement with three extended octagonal ring transducers in each of the three point linkages. The data will be sent and collected by an AM50 Topcon Tierra data logger with GPS localization features and data logger capabilities allowing up to 18 MB logging, thereby assuring the collection of all amounts of data. Each datum is stored with a UTC timestamp. Besides the draught force and GPS co-ordinates, other measurements such as speed, tillage depth and fuel consumption will be taken during the operations. The fuel consumption measurement will be a backup measurement in case there are any problems with the draught force data collection, as the fuel consumption can be related to its values.

Sensor structure located in the three-point-linkage with three extended octagonal ring transducers (left). GPS receptor integrated in the tractor (right).

Both the tractor and the EM38 GPS measurements are made with RTK GPS, i.e. Real Time Kinematics Global Positioning System which is a technique that uses a single reference station for obtaining real-time corrections of the GPS measurements, thus gaining accuracy up to centimeter level. The receiver aligns the two signals, one from the reference station and the other from the GPS. The accuracy of the receiver is a function of its ability to compare the two signals. This makes it more precise than regular GPS measurements and gives very precise location data for the mapping.

Field

The 25 ha field is more or less rectangular, 1000 meters long and around 250 meters wide in average. The field will be worked in perpendicular lines according to its 1000 meters long side. 27 meters of each side will be used as turning area, and any useful data will therefore not be obtained in that area. Furthermore, from the left surface 10% will be set aside in each side for braking and acceleration of the tractor as it is arriving or leaving from the turning area. Only the inner surface of the field will be used for the experiment in that a constant tractor speed is needed such that its variation does not affect the draught force measurements.

EM38

In order to compare the draught forces with the soil type, soil apparent electrical conductivity measurements using an electromagnetic technique (EM38) will be taken, thereby providing location information to the data logger by a global positioning system (GPS). The processed data of the EM38 will be placed on a map and compared with the draught force processed data. These data will also be placed on a map for a visual appreciation of the relation between them. Additionally, the possible

correlation between these two parameters with the statistics values of their linear regression will be studied.

The EM38 method is based on the induction and reflection of the soil's magnetic field, thereby obtaining data, as mentioned, from the electrical conductivity (EC) measured in milliSiemens per meter (mS/m) which is well correlated with the soil texture and its variability across the field (Torp, 2009). Furthermore, the EC brings information about other soil properties such as cation exchange capacity (CEC) which is related to the percent of clay and organic matter (Grisso, 2009) and which is one of the parameters to be measured and correlated with draught force variations. The higher the organic matter and clay content, the higher the CEC. In order to distinguish between organic matter and clay content, measurements at two different depths will be carried out, one at 0 - 30 cm and the other at 30 - 60 cm.

Preliminary studies on building a regional model for calibration of soil organic carbon with diffuse reflectance spectra in a postglacial landscape

Krzysztof Kusnierek, Cezary Kazmierowski*

Department of Soil Science and Remote Sensing of Soils, Adam Mickiewicz University, Poznan, Poland

** kus@amu.edu.pl*

The poster presents the results of the preliminary investigation on building a statistical model for calibration of soil organic carbon (SOC) content using laboratory derived spectral reflectance data by ASD Fieldspec spectrometer in the optical domain. The spectral range between 400 and 2500 nm reveals the chemical composition of a measured target and allows the empirical calibration of a number of soil constituents. Here, the SOC is taken into account. While being the most popular soil constituent to model, it may be also considered as one of the most difficult.

Various soil forming factors influence the bonding of carbon molecules into different humic substances. Therefore, not only the quantity but also the qualitative structure of SOC is revealed by diffuse reflectance spectroscopy (DRS). This introduce an uninformative variance to the calibration model, not to mention the spectral influence of other soil constituents and varying mechanical composition of soils, which also is a reason of reducing the predictive power of DRS to a tool in estimation of SOC content.

While building local SOC calibrations gives the measurement errors comparable to other laboratory techniques (similar soil forming factors) the modeling performed on soils collected on larger areas may produce poor calibration and may require robust troubleshooting.

This work describes the preliminary results on optimizing the performance of the regional SOC calibration model of Poznan Lakeland region. In this postglacial region, the diverse parent material, the geomorphology of the terrain, natural drainage conditions and a short period of pedogenesis result in a very diverse soil cover. The initial dataset was collected to reflect the soil geodiversity of the region and as the statistical model derived from that dataset was not calibrated well, the sensitivity of the model upon the rejection of particular soils and grouping of the samples according to landuse, soil type and soil texture was investigated.

Nordic Association of Agricultural Scientists

Contact: NJF General Secretariat

E-mail: njf@njf.nu
Website: www.njf.nu
ISSN 1653-2015